

ADF Imager

P. Stadelmann
jems-swiss
Chemin Rouge 15
CH-1805 Jongny
Switzerland
info@jems-swiss.ch

December 3, 2020

Contents

1	Introduction	3
2	Models	6
2.1	Graphene	6
2.2	III-V semiconductors	7
3	Controls	14
3.1	Iteration tab	14
3.2	Multislice tab	17
3.3	Options tab	19
3.4	Scanning tab	19
3.5	Signal tab	21
4	Image tabs	25
4.1	Bright-field image tab	25
4.2	Dark-field image tab	27
4.3	Sector images tab	28
4.4	Sectors image tab	30
4.5	Model slices tab	31
4.6	Projected potential tab	32
4.7	Absorption potential tab	33

4.8	Fresnel propagator tab	34
4.9	Phase-object tab	36
4.10	Power spectrum tab	37
4.11	Bright-field detector tab	38
4.12	Dark-field detector tab	39
4.13	Sectors detector tab	40
4.14	Wave-function tab	41
5	Probe imager dialogue	42
5.1	Scan area and probe position	43
6	Setting the bright-, dark-field and sectors detectors	45
7	Doing a bright- or dark-field and sectors image calculation	47
8	Example: GaAs [110]	49
9	Notes	53
9.1	Note 1: Debye-Waller temperature factor	53
9.2	Note 2: calculation of the atomic scattering amplitude	54
9.3	Note 3: absorption coefficient μ_{TDS}	54
9.4	Note 4: popup menu attached to slider controls	54
9.5	Note 5: sampling artefacts	55

1 Introduction

ADFIImager dialogue (Fig. 1) is used to calculate STEM bright-field (BF), dark-field (DF) and sector-bright- or sector-dark-field (SE) images¹.

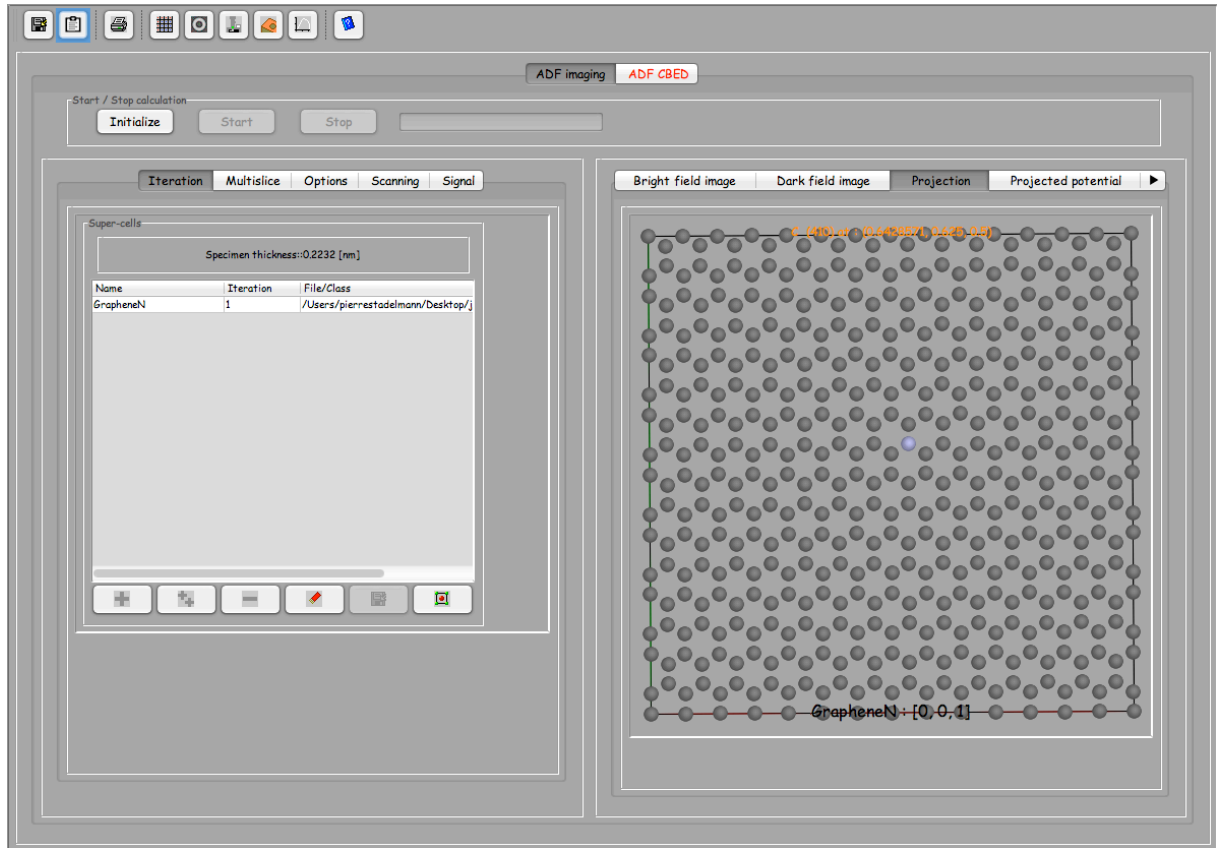


Figure 1: STEM images, annular dark-field, bright-field images or sector-bright- or -dark-field images are calculated using the ADFImager dialogue.

The controls and calculated images are grouped in 2 tabs. The model crystal is described as slices in the left tab (**Iteration**, ...), the generated BF, DF or SE images are displayed in the right tab (*BF, DF SE, images, model, ..., detectors, wave-function*).

The tool buttons of Fig. 2 allow to:

1. Save the ADFImager dialogue.

¹jems version 4.3906u2016 or later.

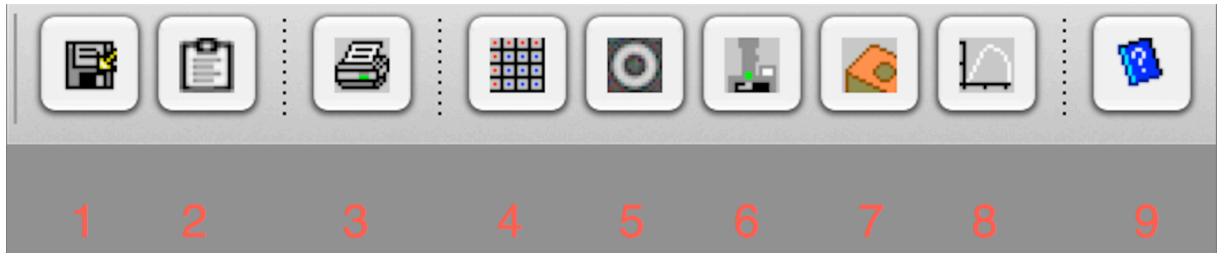


Figure 2: Tool buttons of the ADF imager dialogue.

2. Transfer the ADFImager dialogue to the clipboard (for documenting the calculations).
3. Print the ADFImager dialogue.
4. Tabulate the bright- and dark-field images or thickness series (stack) of BF/DF images.
5. Adjust the bright- and dark-field detectors radii.
6. Select a microscope and set the probe aberrations, i.e. defocus, astigmatism. Aberrations up to order 8 can be accounted for.
7. Select specimen related parameters.
8. Display the optical transfer function, probe shape and Ronchigram.
9. Display the ADFImager dialogue help.

The calculations are initialized, started and stopped using the buttons of Fig. 3. The **Initialize** button (1) generates the projected potential of all the slices at once as well as the phase-object function (PO). The Fresnel propagator (FP) of all the slices of the model are initialized when needed during the calculations. Calculation time is saved when all the slices have the same thickness. The **Start** and **Stop** buttons starts and stops the ADF calculation respectively.

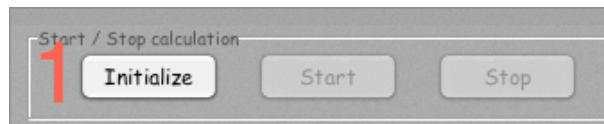


Figure 3: Initialize, Start and Stop buttons. Initialize button (button 1) should be pushed after setting the ADF image calculations parameters.

Note that a popup menu is attached to every drawing or image. Popup menus are displayed as usual (mouse right-click or by a mouse double click). On a touch

screen have the finger stays longer on the control. Popup menus allow to print, save or send the drawing or image to the clipboard.

2 Models

2.1 Graphene

One of the models that are employed in this document is a **graphene** sheet where one carbon atom has been replaced by a nitrogen atom. With this model calculations are performed within minutes (Fig. 4). The graphene model is made of atoms placed at (x, y, z) coordinates in an orthogonal box of sides a, b, c with $0 \leq x, y, z < 1$. Note that the model is projected along the Oz direction $([0,0,1])$ parallel to \vec{c} . It is best to have a tetragonal model, i.e. with $a = b$, since this allows a faster display of the generated images and power spectra.

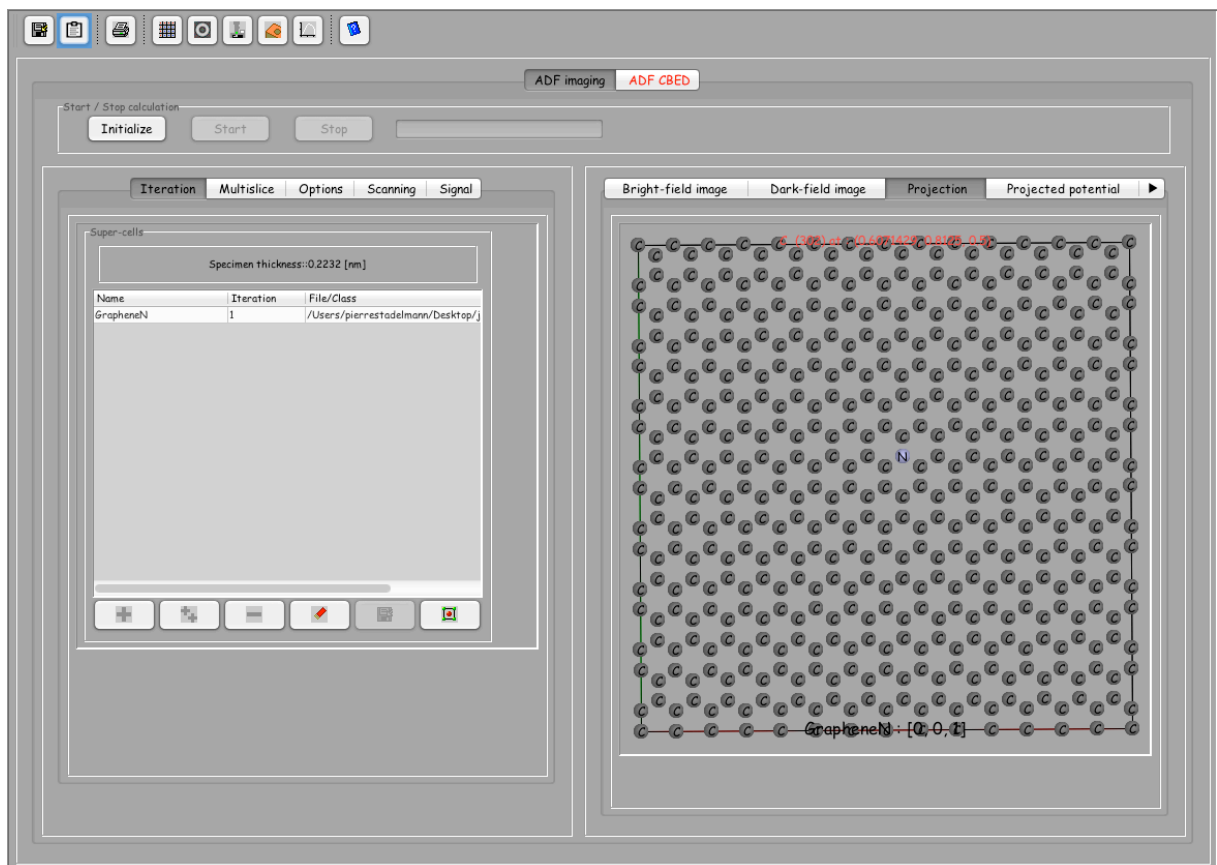


Figure 4: Graphene model with labelled atoms. Labels are obtained using the popup menu attached to the projection. Popup menus are shown when the mouse is positioned on the drawing or table and a double click is issued.

Thicker crystal models should be prepared as series of slices. This is easily achieved

using tools provided by the **Miscellany** menu. Electrons are traveling from top the slice (somename_0000.txt) to the bottom slice (somename_nnnn.txt). The slices thickness does not have to be identical².

2.2 III-V semiconductors

The calculation of [110] bright-field, dark-field or sector images of III-V semiconductors (AlAs, AlP, AlSb, GaAs, GaP, GaSb, InAs, InP, InSb and ZnTe) requires to transform the cubic unit cell (space-group $F\bar{4}3m$) into an orthorhombic unit cell of c axis || to the cubic [001]. The procedure is as follow (the example uses ZnTe):

1. Open the ZnTe model (Fig. 5). Verify the atom coordinates, occupancy and Debye-Waller temperature factor.
2. In menu *Crystal* select menu item *Make orthogonal* (Fig.8). Note that the orthogonal unit cell can be pretty large and also that orthogonality can't always be achieved perfectly (there is a tolerance of 0.2 degree).
3. After selecting the [110] direction, close the specimen dialog (). The right tab of the dialog will then show the orthogonal unit cell and its geometrical relationship with the ZnTe unit cell (Fig. 9). Note that the new cell $[uvw]$ directions and (hkl) indices are given with respect to its own metrics. The space-group is the new cell is set to $P1$.
4. Using 3-D display, it is easy to see that the new unit cell is doubled in the [001] direction (Fig.10). In this particular case, it would be possible to keep only a half unit cell (menu *Miscellany* menu item *To slices*).
5. The generation of super-cells is made possible by several menu items grouped in the *Miscellany* menu. Since the new orthogonal unit cell must be cut in thinner sub-slices in order to perform BF, ADF or SE image simulations, the dialog attached to the *To slices* menu item is activated (Fig. 12). This dialog allows one to duplicate a cell in $[100]_x, [010]_y$ or $[001]_z$ directions and to cut it into thinner sub-slices parallel to either Ox, Oy or Oz.
6. For ADF image simulation it is better to generate approximately square super-cells. This is achieved here by duplicating the cell 5 times along Ox and 7 times along Oy (Fig.13), a, b, c have length 4.377, 4.333 and 0.875 nm respectively.

²Though a single slice thickness requires less computer memory.

7. The cell is finally sliced in 4 sub-slices perpendicular to Oz using the popup menu attached to the table. A slice thickness of 0.2 nm is appropriate. After slicing and saving the sub-slices (give the sub-slices a meaning full name, for example ZnTe110) close the *To slices* dialog. The subslices are named *ZnTe110_0000.txt*, ..., *ZnTe110_0003.txt*.
8. Finally open subslice *ZnTe110_0000.txt* (Fig. 14).

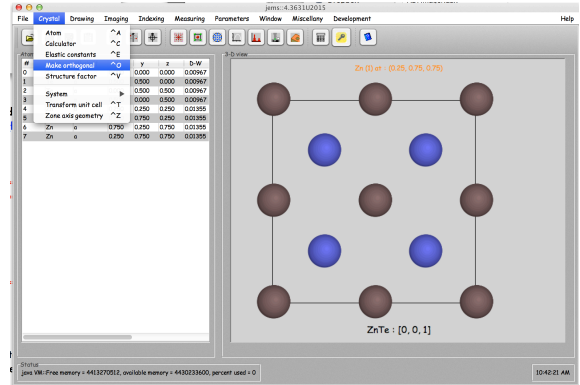
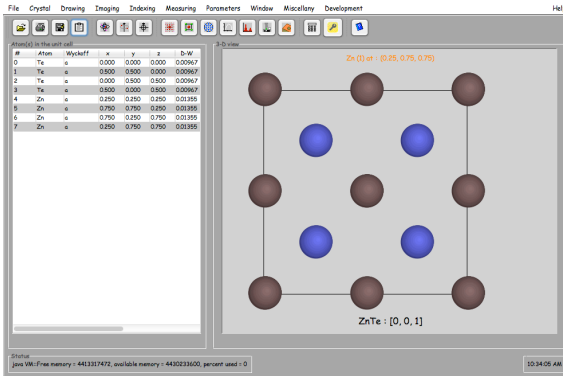


Figure 5: ZnTe model. Te atom at (0,0,0) and Zn at $(\frac{1}{4}, \frac{1}{4}, \frac{1}{4})$.

Figure 6: Make orthogonal generates orthogonal units cell with c axis || to any $[uvw]$ direction the selected crystal.

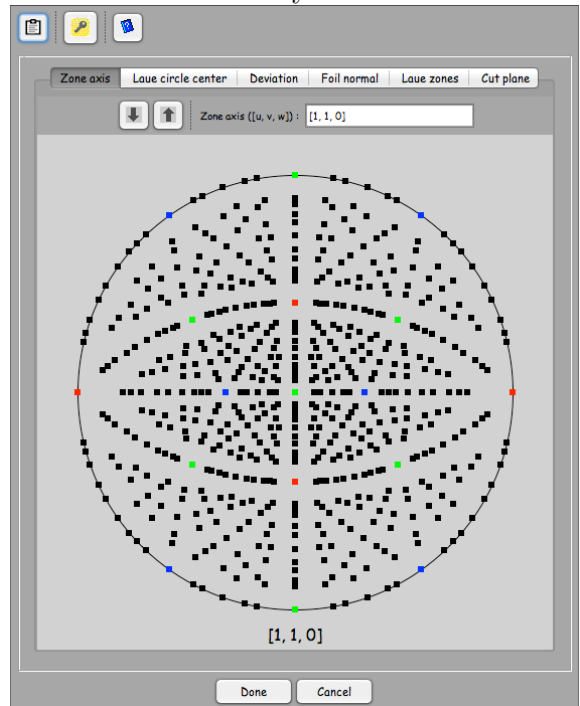
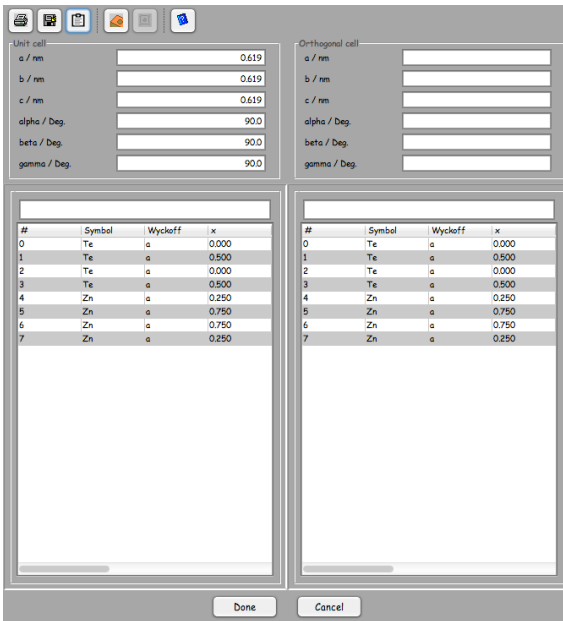


Figure 7: Make orthogonal dialog. The left tab shows the original unit cell, the right tab the specimen dialog (toolbutton 1, Fig.7). will show the orthogonal unit cell after selecting a $[uvw]$ direction. By default the $[001]$ direction is selected (i.e. left and right tabs show the same structure).

Figure 8: A $[uvw]$ direction is selected using zone axis tab.

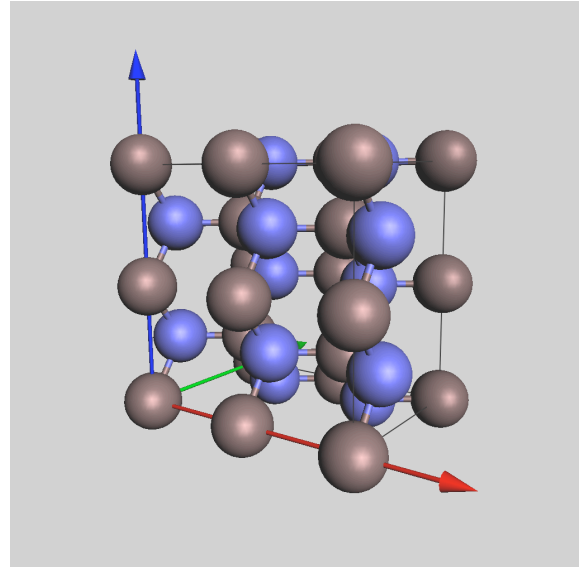
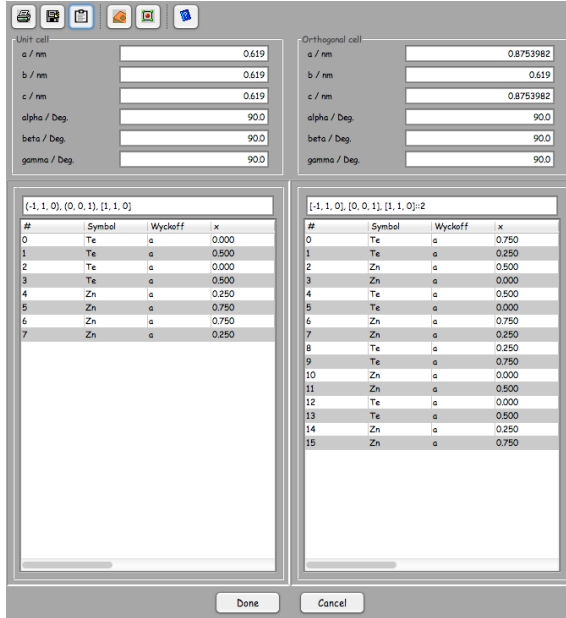


Figure 9: The orthogonal unit cell has $[001] \parallel [\bar{1}\bar{1}0]_{ZnTe}$, $[010] \parallel [001]_{ZnTe}$ and $[001] \parallel [110]_{ZnTe}$. Its unit cell volume is twice the volume of ZnTe.

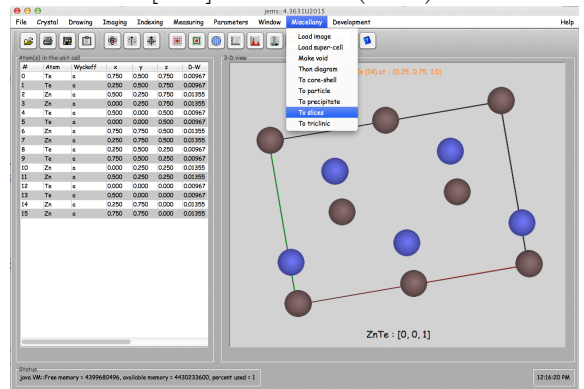
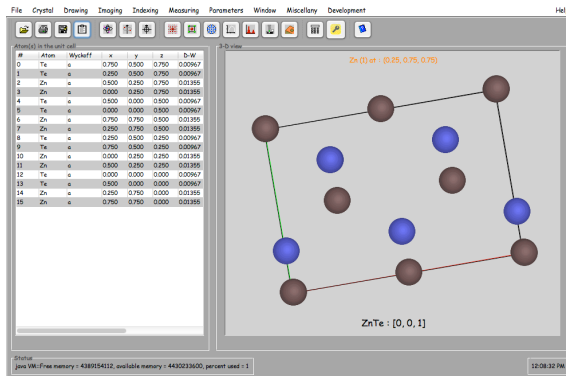


Figure 11: After closing the *Make orthogonal* dialog a $[001]$ projection is shown as well as sliced using menu *Miscellany*, menu item *To slices*.

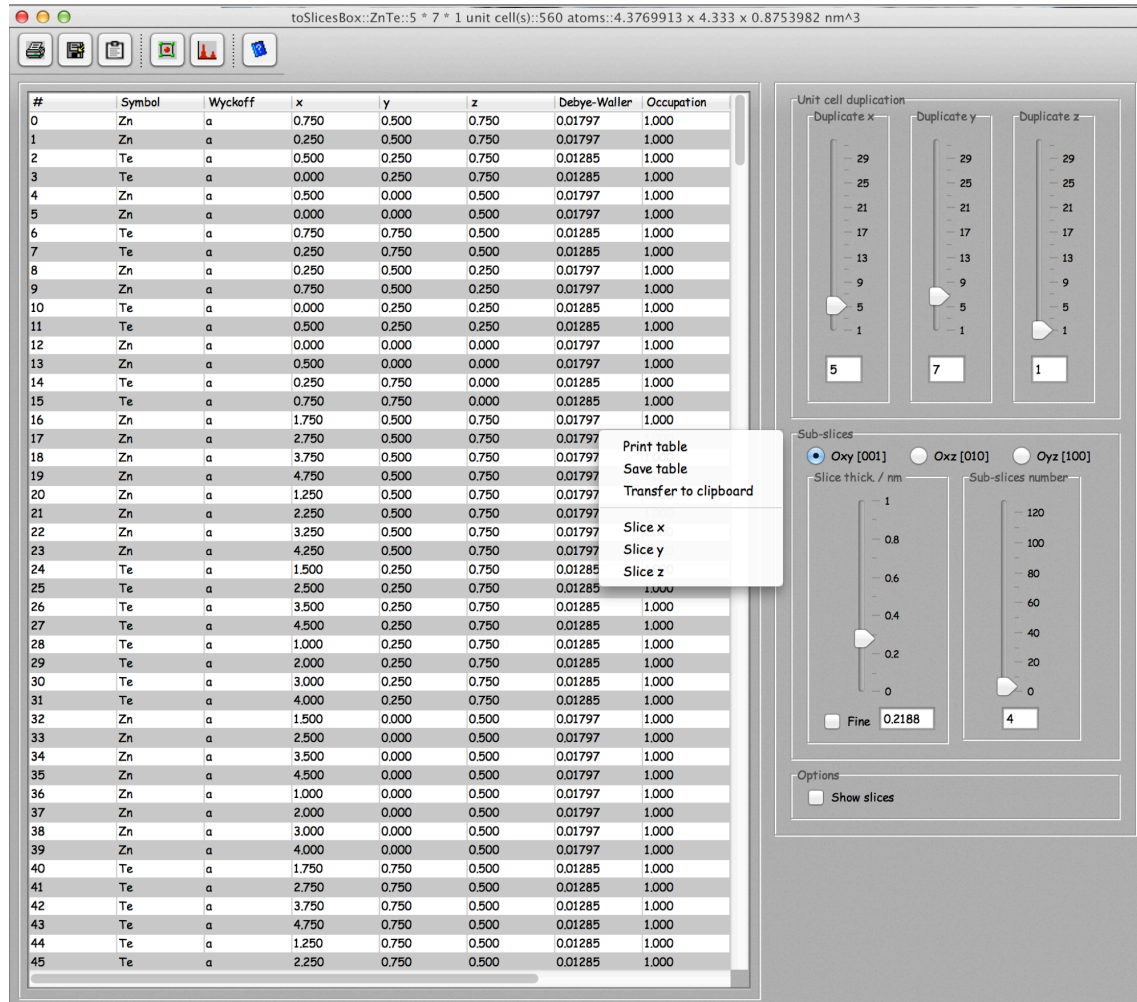


Figure 13: The orthogonal unit cell is duplicated 5 times in Ox direction (a) and 7 times in Oy direction (b). The new lattice parameters show that the super-cell is nearly tetragonal (when lattice parameter a and b are almost equal, all the images shown during the ADF image calculation will have their proper geometry (some are not interpolated before they are displayed in order to speed up simulations)).

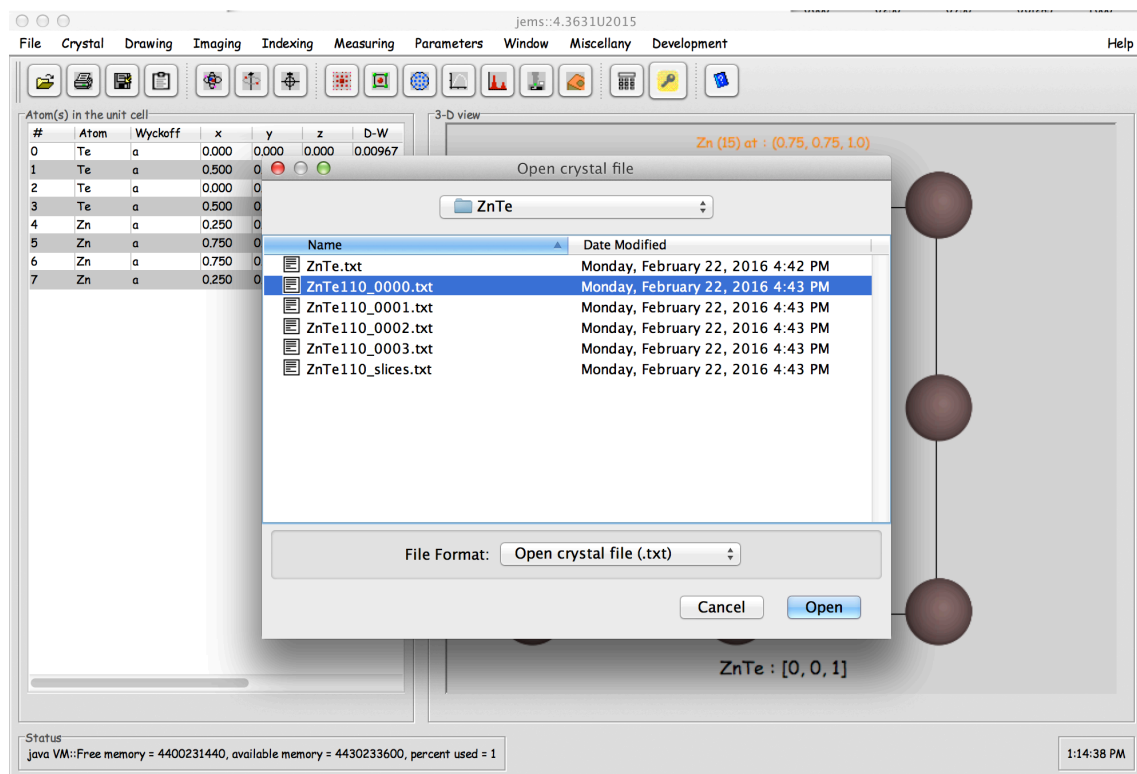


Figure 14: The original ZnTe folder now contains the ZnTe cubic unit cell, 4 super-cells (subslices) and the whole unsliced super-cell (ZnTe110_slices.txt).

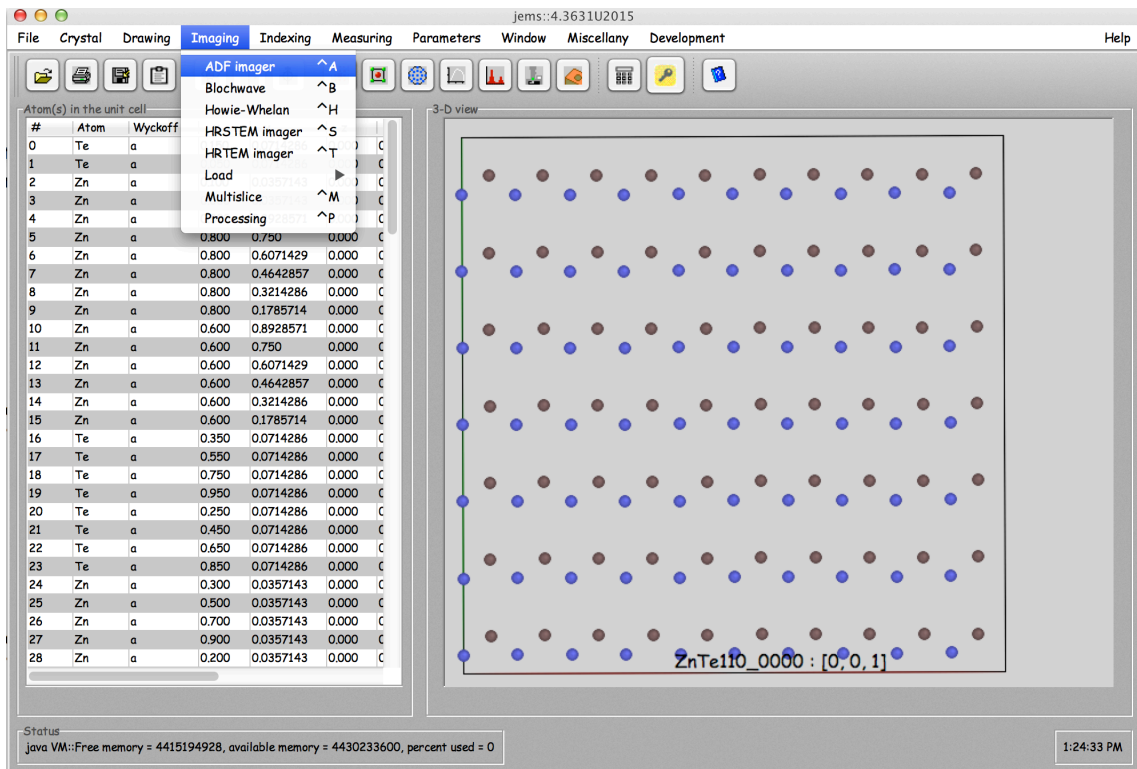


Figure 15: The ADFImager dialogue is found in the *Imaging* menu.

3 Controls

3.1 Iteration tab

The buttons of the **Iteration** tab (Fig. ??) allow to control the stack of slices describing the model³. Slice numbered *somename_0000.txt* is the top slice of the stack. Buttons 1 to 6:

1. Load one slice of the model.
2. Load a series of slices (numbered *somename_0000.txt*, *somename_0001.txt*, ..., *somename_9999.txt*)⁴.
3. Suppress the slice that is selected from the stack.
4. Suppress all slices.
5. Save the series of slices.
6. Display a 3-D view of the model.

The total specimen thickness. i.e. the cumulated thicknesses of all the slices is displayed (Fig. 16). The maximum number of slices is 10'000. Note also that a **popup menu** is attached to the table of slices that allows to duplicate the stack. It is also possible to remove or add single super-cells in order to select a particular total crystal thickness.

³Only slices in jems .txt format are accepted.

⁴A maximum of 10'000 slices is considered.

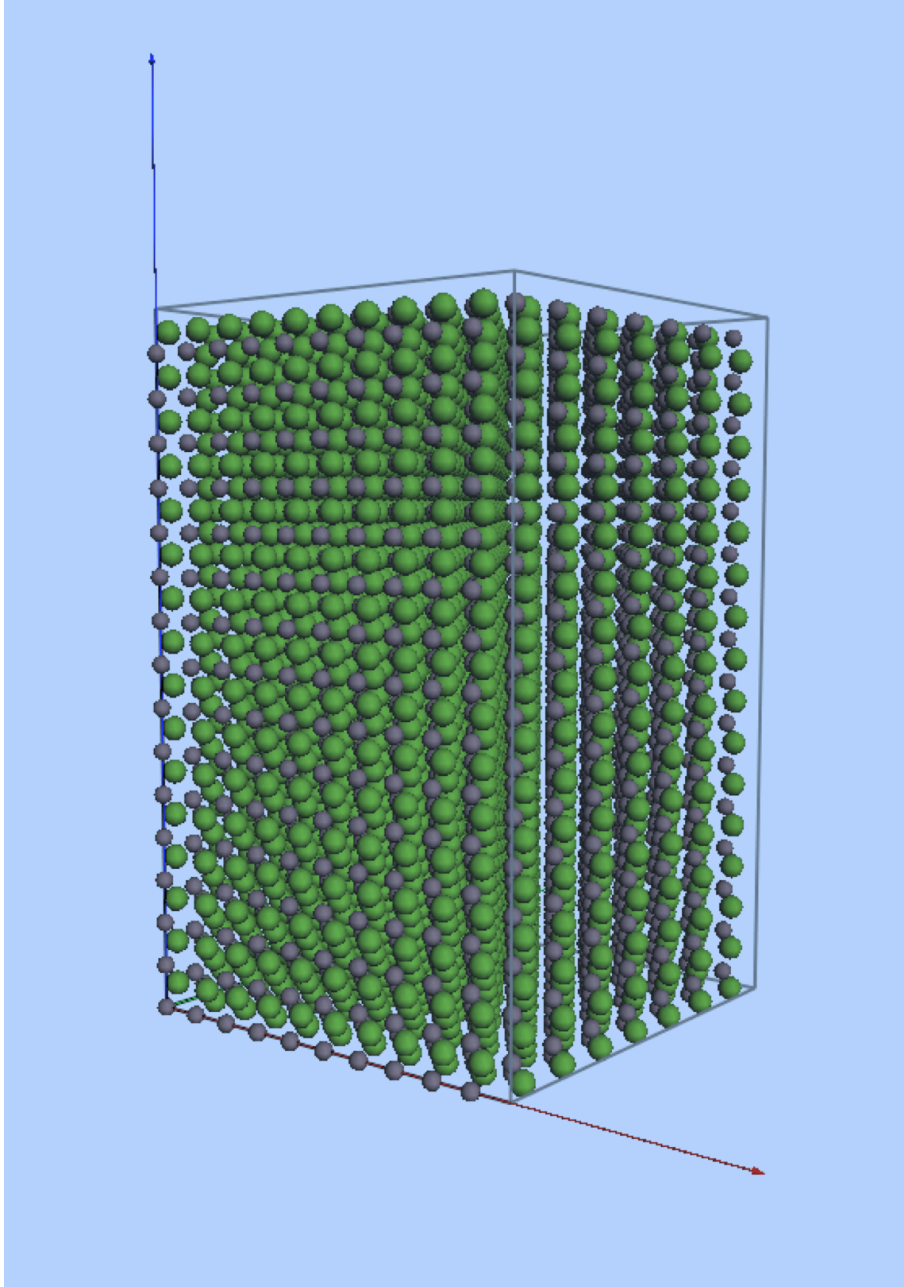


Figure 17: 3-D view of the model reconstructed using the super-cells.

3.2 Multislice tab

The controls of the multislice tab are shown in Fig. 18. The `Reset` button resets the calculation of the phase-object function of all the slices.

The controls are grouped in 5 boxes that allow to:

1. Select the method employed to generate the projected potential of the slice. The `Fourier` method generates the potential in Fourier space. It is the most precise, but also the slower. The `Analytic` method uses an analytic form of the projected potential of the atoms at their (x, y) position, it is selected by default and is slower than the direct one. The `Direct` method generates the slice projected potential by patching the projected potential of the atoms at their (x, y) position in the slice. It is the fastest method and less precise one (see note 9.2). It can result in square patterns in the ADF images of thick crystals.
2. Define the sample size. The sample size is directly related to the maximum scattering angle (given in the **tool tip text**. The maximum scattering sets the default outer radius of the *annular dark-field detector*⁵. When (N_x, N_y) samples are used, the maximum scattering angle is:

$$q_{max} = \text{Min} \left(\frac{N_x}{2a}, \frac{N_y}{2b} \right)$$

In order to cancel aliasing errors due to convolution the Fresnel propagator is band limited to $\frac{2}{3}q_{max}$.

3. Define the multislice precision `$O(\Delta z)$` or `$O(\Delta z^2)$` and to take absorption into account. `Absorption` is better introduced when using Wieckenmeir-Kohl atomic scattering factors (`WKc`) of the Options tab.
4. Define the potential or image interpolation method and enable the lattice vibration at a selected temperature. The Debye-Waller temperature factor is adjusted according to the temperature value (linear approximation). Uncorrelated (Einstein model) atomic vibrations model is used (frozen lattice, see note 9.1).
5. Repeat the whole calculation using a new configuration of atoms (frozen lattice). 5 configurations are often sufficient to obtain significant BF, ADF or SE images.

⁵The tool tip text of any control is displayed when the pointer (or mouse) rests 2 seconds on the control

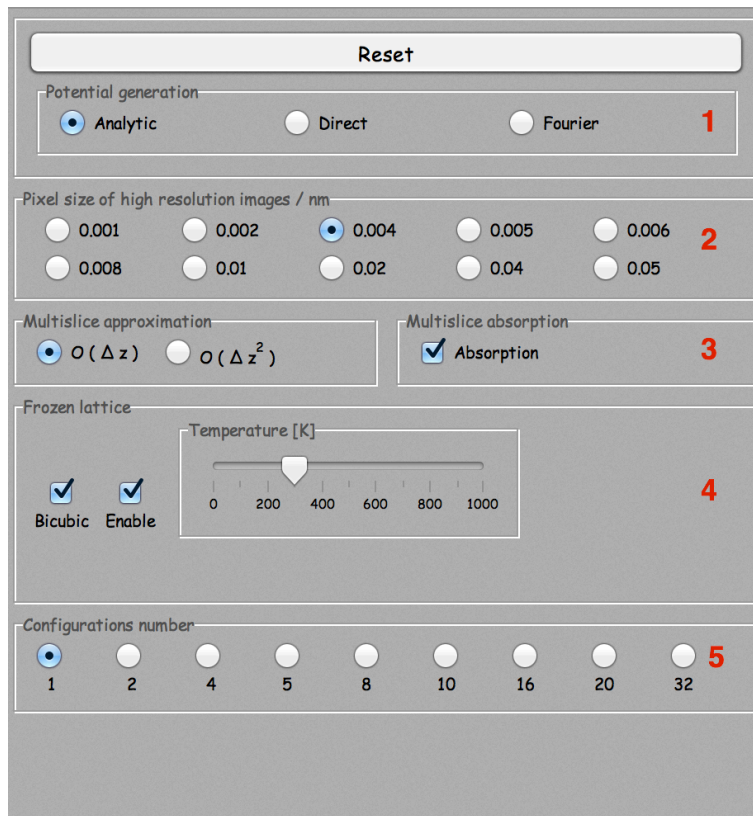


Figure 18: Multislice tab. The **Reset** button erases the pre-calculated slice potential arrays of the whole stack of slices.

3.3 Options tab

The controls of the **Options** tab (Fig. 19) are grouped in 6 boxes. Box number:

1. Select the source of the atomic form factors. It is, in principle, best to use the *Weickenmeier-Kohl* tabulation (WK or WKc) since it doesn't describe the atomic form factor as a sum of gaussian functions and introduces absorption using the Debye-Waller temperature factor (see note 9.2).
2. The ADFImager allows to specify 4 different Bright-field, Dark-field or Sectors detectors at once. The different channels (Bright-field, Dark-field or Sectors) are selectable (and not need to be all selected) and when calculating images for more than one configuration (Frozen lattice), the images can be saved automatically (Save)⁶
3. Select a calculation method⁷.
4. Select the unit cell crystal that has been duplicated to generate the super-cells and the [uvw] orientation with respect to it. In this example GaAs and zone axis [110] are specified in order to have the diffraction patterns drawn when selecting the detectors acquisition angles with the ZnTe cubic structure not the super-cells.
5. When the model is made of several slices, the BF, DF and SE images after each slice are saved as a stack of images. The BF/DF/SD progress checkbox allows to follow the progress of the calculations⁸.
6. Display the BF, and SD detectors outer and inner-outer radii.

3.4 Scanning tab

The controls of the scanning tab (Fig. 19) are grouped in 6 boxes:

1. Allow to introduce masks that attenuate aliasing and sampling artefacts introduced by the discrete nature of the multislice calculation (see note 9.5).

⁶The different channels are saved in different folders that are named using the scheme **Conf n BF m** where **n** is the configuration number and **m** the detector number.

⁷Only the Frozen lattice method is available in jems version 4.

⁸Images can be displayed after a given percentage of the scan has been performed. The percentage is selected in the **Scanning** tab.

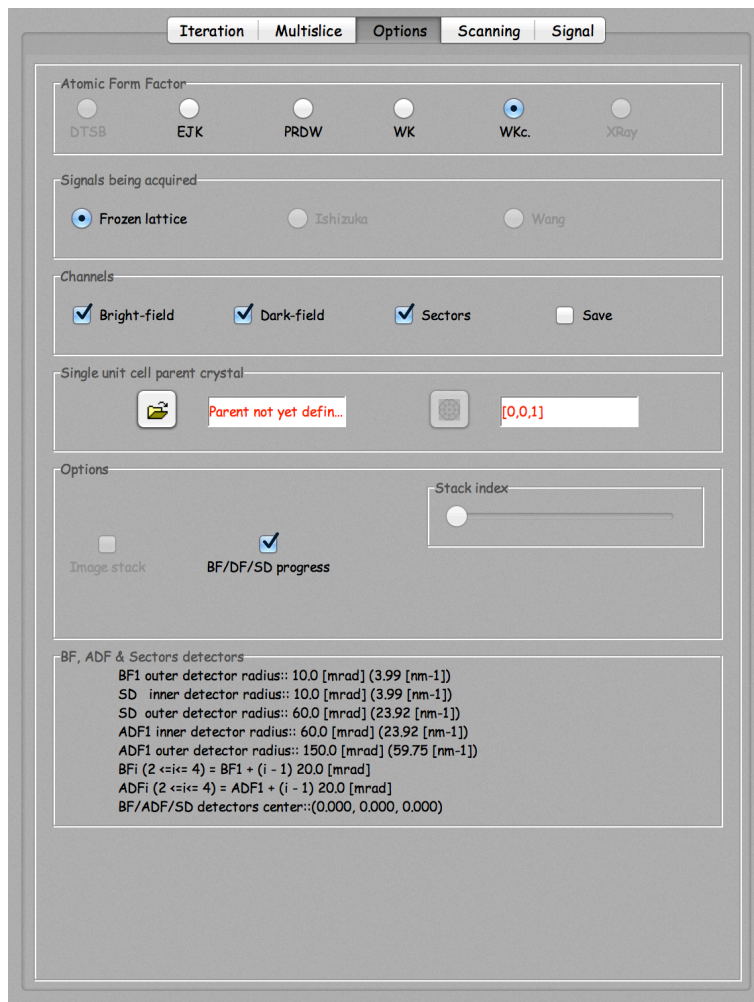


Figure 19: Options tab. The BF,DF or SD detectors radii are provided in box 5. These radii can be adjusted when the calculation is running. There is a fixed selectable radius increment for the BF and DF detectors.

2. Define the size of the multislice calculation. The different **Radiobuttons** are enabled according to the pixel size selected in the **Multislice** tab.
3. Define the size of the scanned area. It is usually better to start a new calculation using a small scan area size and a large **Scan step size**. The calculation will be faster since not all scan points are taken into account.
4. Allow to mask some artefacts of the multislice calculation⁹. The artefacts are imaged using a large *Power spectrum logarithm scale*. When masked the DF detector area is reduced¹⁰. These artefacts are of several possible origins (Fig.21:
 - (a) Too coarse super-cells sampling, the projected potential displays discontinuities.
 - (b) too coarse multislice size, aliasing effects start to be important. Increase the multislice size or introduce a mask and/or cross-mask.
 - (c) Use the Direct method to generate the projected potential of the slices.
 - (d) Accumulation of rounding errors during the multislice calculations. Note that they only are appearant when a very large logarithm scaling factor is employed to display the power spectrum and the intensity on the detectors. These artefacts only appear for thick crystal.
5. change the rate of refreshing the BF, DF or SD images.

3.5 Signal tab

The **Signal** tab controls the BF, DF or SD signals intensity and change the brightness, contrast and gamma of the BF and DF images (Fig. 22). The last set of *radiobuttons* changes the multiplication factor (**a**) that is introduced when power spectrum images are displayed using a logarithm scale:

$$\text{displayed intensity} = \log [1 + a \times \text{signal intensity}]$$

It is equivalent to increase the signal gain by a factor of 10^n .

The pixels value of the BF and DF images do not use a logarithm scale. They are given by:

⁹These artefacts are of very small amplitude, usually 10^2 to 10^6 smaller than inelastic scattering intensity for very thin models. For models made of very light atoms, they can be larger. They are made more visible when the inner radius of the DF detector is large

¹⁰The reduction is displayed in the jems console.

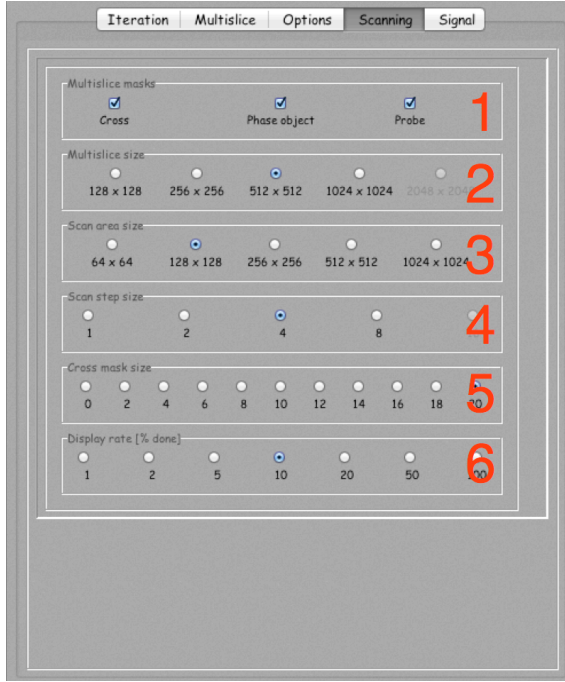


Figure 20: Scanning tab.

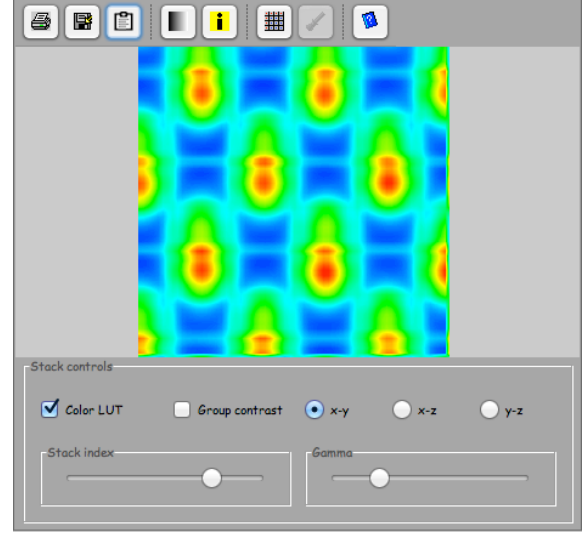


Figure 21: ADF artefacts.

- Bright-field (BF):

$$BF_{pixel\ value} = BF_{signal\ integrated\ on\ BF\ detector} \times BF_{gain}$$

- Dark-field (DF):

$$DF_{pixel\ value} = DF_{signal\ integrated\ on\ DF\ detector} \times DF_{gain}$$

- Sector detector (SD): The four sectors have the same gain.

$$SD_{pixel\ value} = SD_{signal\ integrated\ on\ Sd\ sector} \times SD_{gain}$$

For a $100\ pA$ incident probe intensity, the DF signal intensity will be $100\ pA \times \frac{1}{DF_{gain}}$.

Image brightness, contrast and γ correction are modified using Brightness, Contrast, Gamma. This is possible only when the simulation is finished. Changing the signal gain will introduce bright or dark lines in the images.

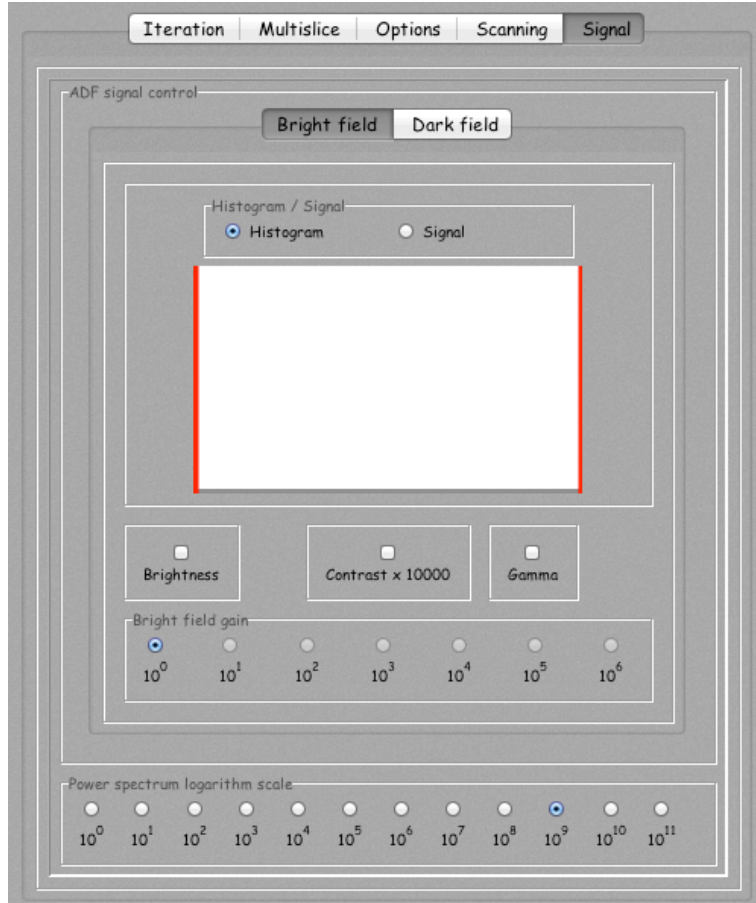


Figure 22: The BF, DF and SD signal intensity is provided by integrating the power spectrum intensity over the BF, DF or SD detectors. Finally the integrated values are multiplied by the BF gain (default is 1), DF gain (default is 10^9) or SD gain (default is 10^3) respectively. The incident probe intensity is initialised to 1.

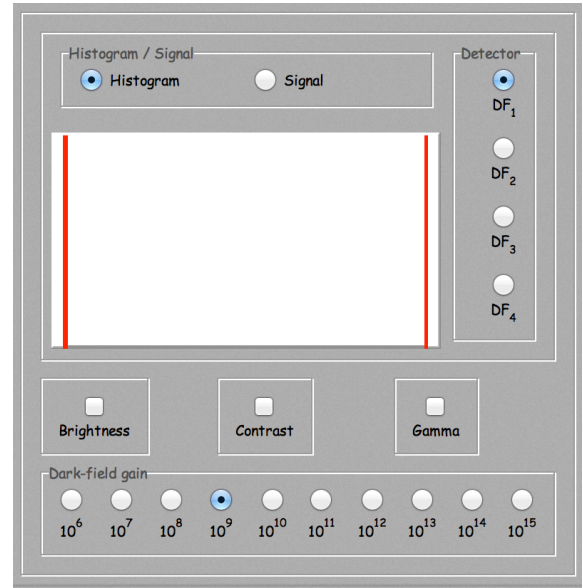
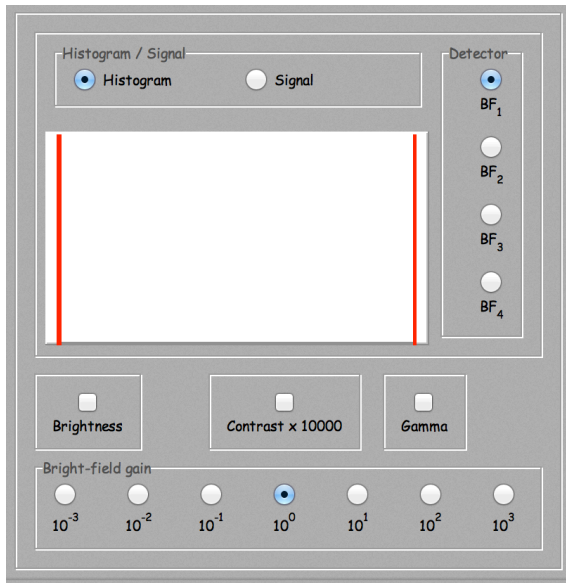


Figure 23: The BF channel (BF1,..., BF4) can be selected during the simulation and the intensity is displayed in the corresponding result tab. Figure 24: The DF channel (DF1,..., DF4) can be selected during the simulation and the intensity is displayed in the corresponding result tab.

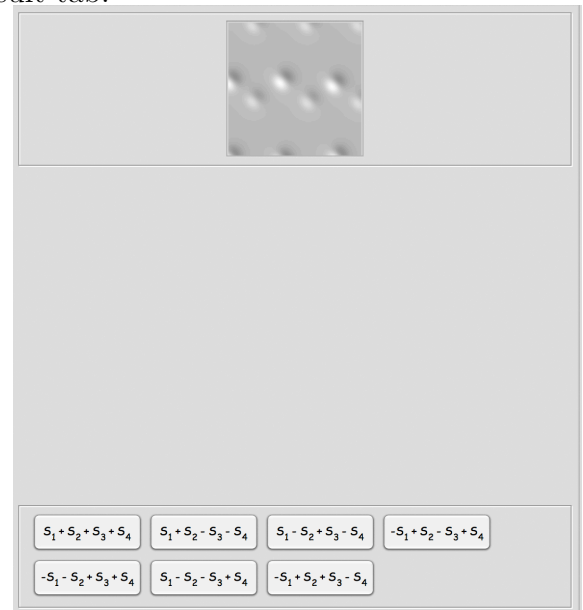
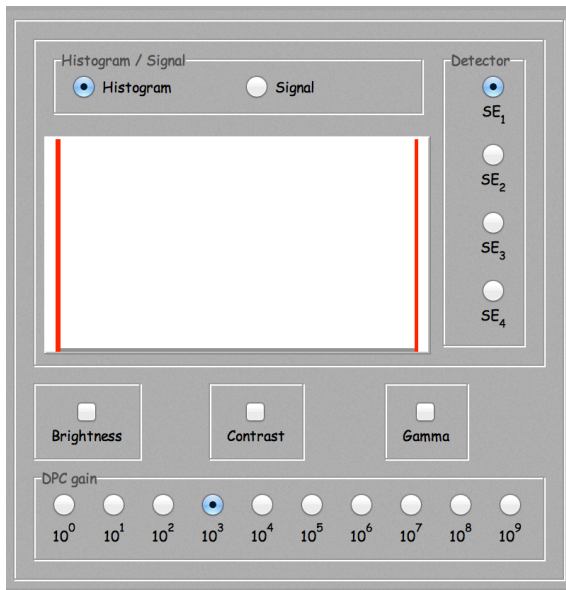


Figure 25: The signal intensity of any one of the 4 channels SE1,..., SE4 can be selected and displayed in the corresponding panel. When the calculation ends these channels can be added and/or subtracted in order to produce differential contrast images.

4 Image tabs

4.1 Bright-field image tab

The scan of bright-field, dark-field or SD images is performed twice (Fig. 27). The first one starts at pixel ($x = 0, y = 0$) and continues at pixel $(2, 0)$, i.e. even columns first, while the second one starts at $(1, 0)$ and continues at $(3, 0)$, i.e. odd columns second. In this way BF, DF or SD images are displayed almost immediately. In order to obtain faster **complete calculations** it is indeed necessary to set the **Display rate** to 100 % or to uncheck the **BF/DF progress** of the **Options** tab.

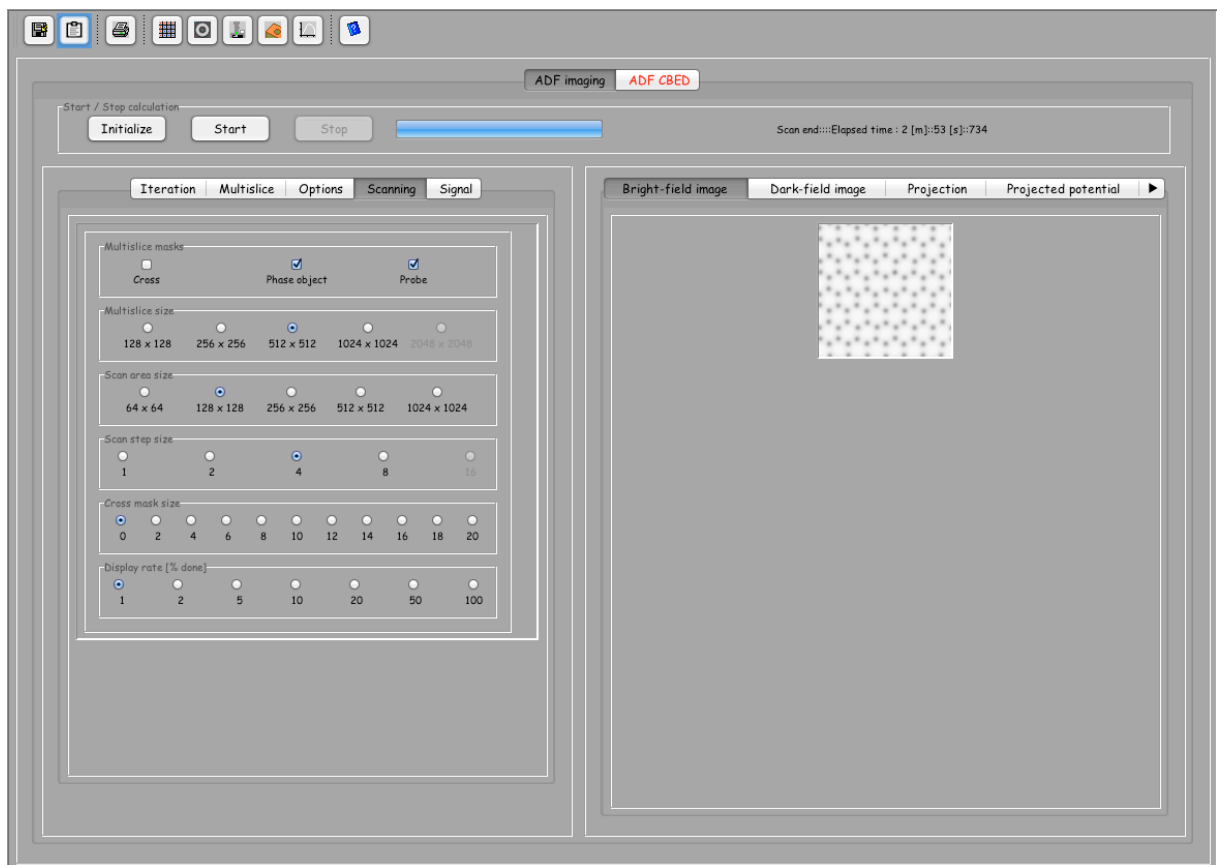


Figure 27: Bright-field image tab.

When using a small **Scan area size**, the first scan position is ($x = 0, y = 0$) and the next is $(n \times 2, 0)$ where n is the **Scan step size**. Calculated images are smaller by a factor n , but can be tabulated and displayed interpolated to a

dimension given by ($Scan\ area\ size \times Step\ size$) (Fig. 28 and 29)¹¹.

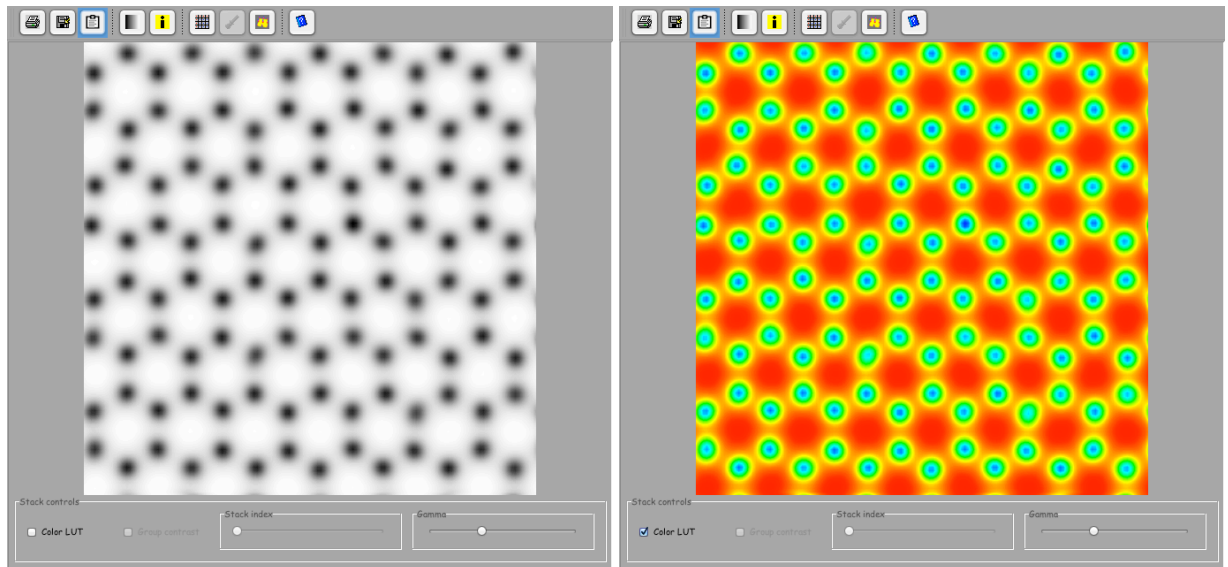


Figure 28: Interpolated gray scale bright-field image (512×512).

Figure 29: Interpolated coloured bright-field image (512×512).

Interpolation produces images of size ($scanSize_x \times scanStep_x, scanSize_y \times scanStep_y$).

¹¹Use tool button 4 to tabulate BF, DF or SD images.

4.2 Dark-field image tab

The calculation of the dark-field images is performed in parallel to the bright-field images¹² (Fig. 30).

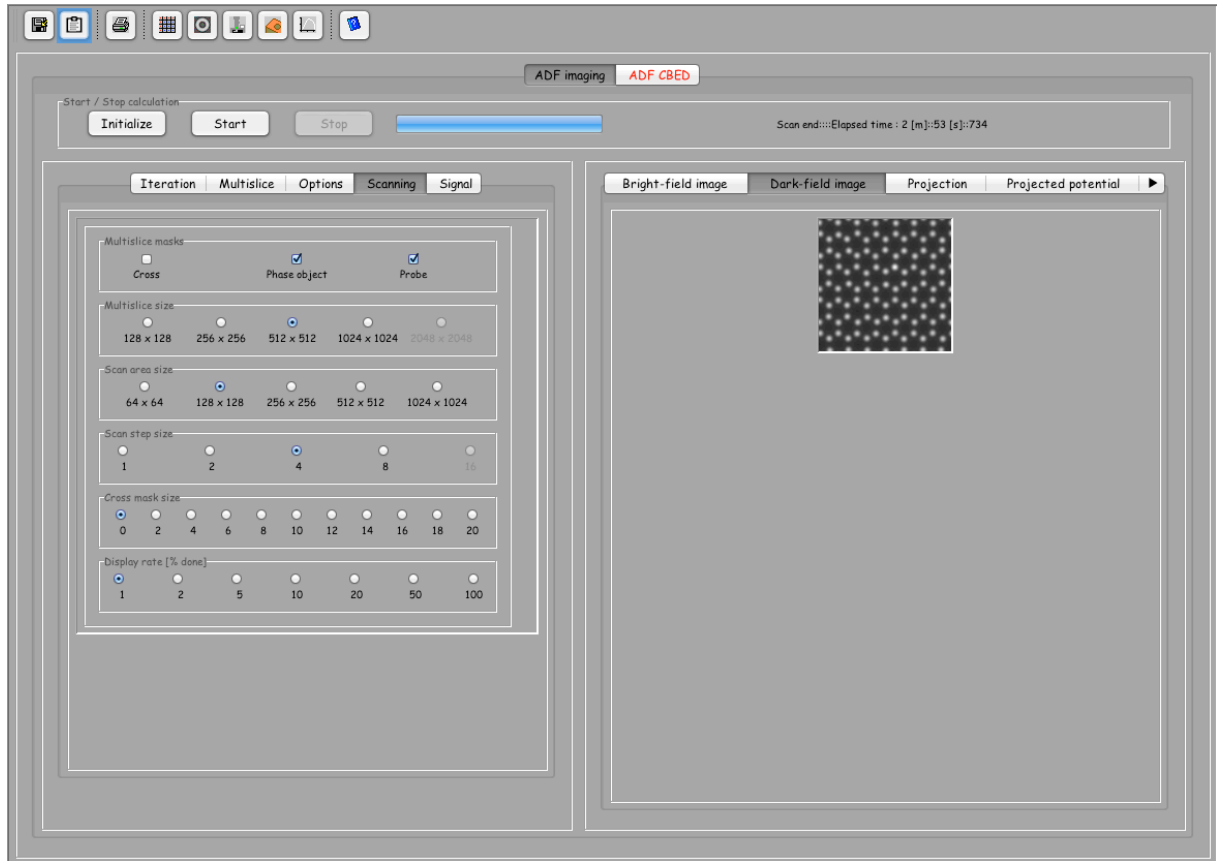


Figure 30: Dark-field image tab displays the DF image when a given percent of the calculation has been performed (*Display rate*).

The DF image is tabulated, using tool 4 (Fig. 2) and displayed interpolated as shown in Figs. 31 and 32.

¹²Use tool button 4 to tabulate BF and DF images.

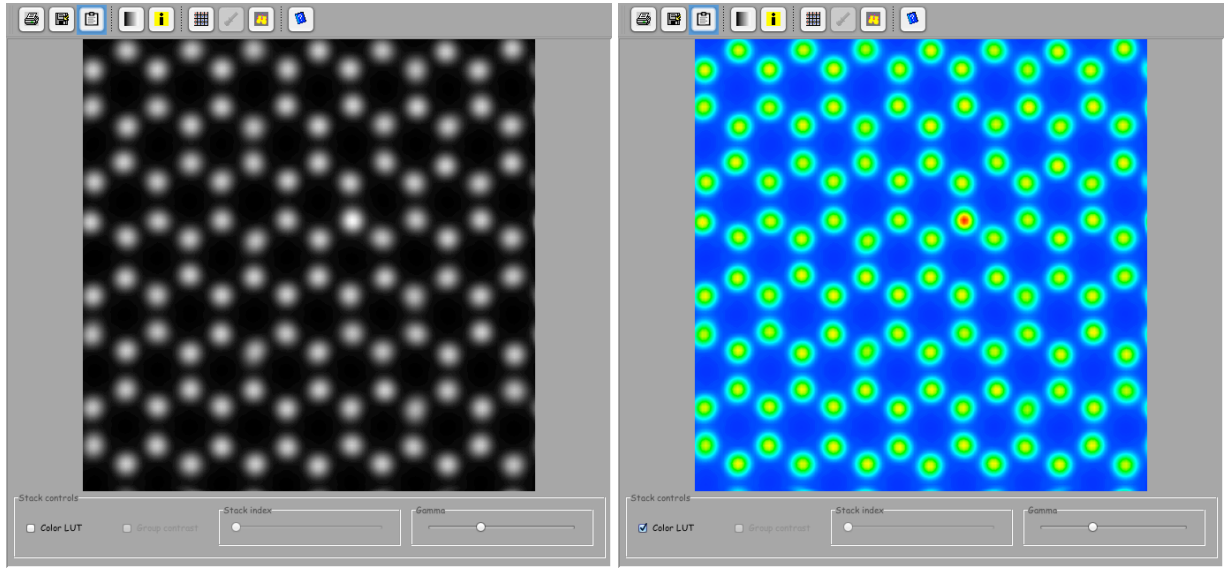


Figure 31: Interpolated gray scale dark-field image (512×512).

Figure 32: Interpolated coloured dark-field image (512×512). Note that the N atom contrast.

4.3 Sector images tab

The calculation of the 4 sectors images is performed in parallel to the bright-, dark-field images¹³ (Fig. 33). During the calculations the sector that is being displayed is selected in the **Signal tab**.

After completing the simulations, the different sectors images (S_1, \dots, S_4) can be added or subtracted using the 7 buttons at the bottom of this image tab. For example $\boxed{S_1 + S_2 + S_3 + S_4}$ will add the images of the 4 sectors (it will then be either a BF or DF image).

¹³Use tool button 4 to tabulate BF, DF or SD images.

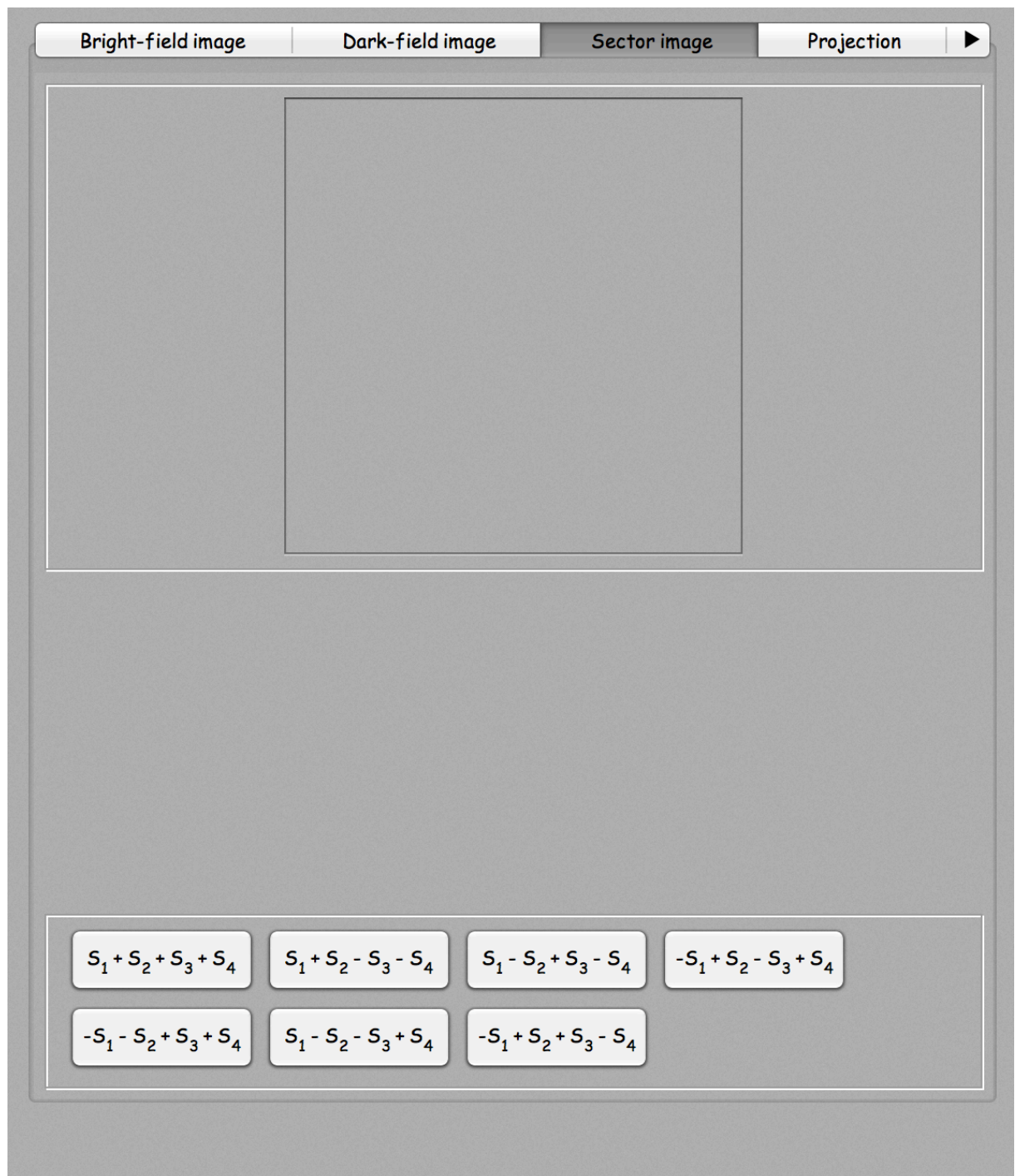


Figure 33: Sector image tab displays the Sector image when a given percent of the calculation has been performed (*Display rate*).

4.4 Sectors image tab

The sector detector is divided in 4 quadrants S_1 (top right), S_2 (top left), S_3 (bottom left) and S_4 (bottom right). Their intensity content can be added and/or subtracted in order to obtain differential phase contrast images (Fig.34).

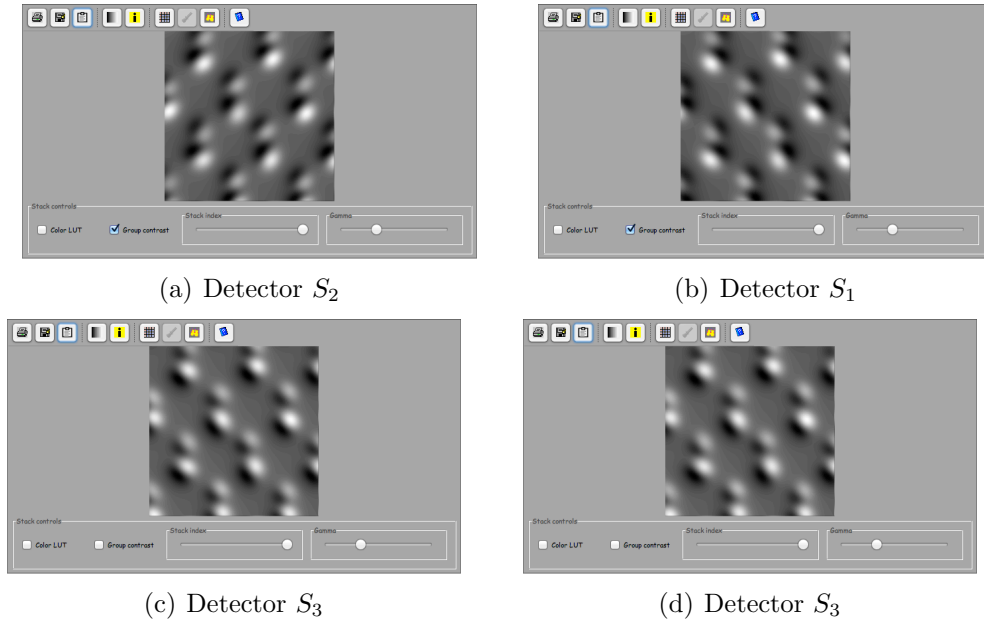


Figure 34: Quadrant detectors

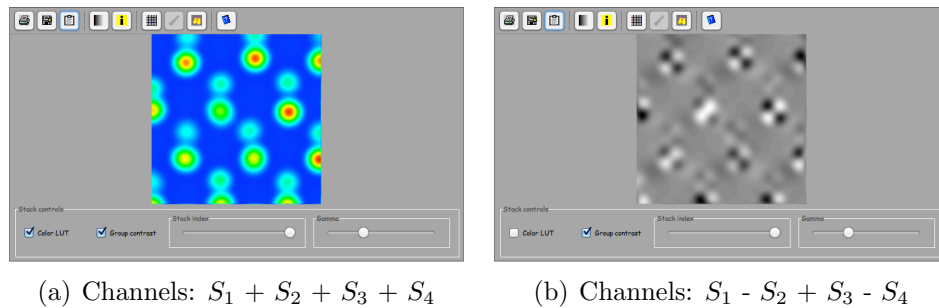


Figure 35: Channels sum and DPC image.

4.5 Model slices tab

Any slice when selected can be displayed in this tab (Fig. 36). The atoms displacement are not shown on the model drawing, but on the projected potential images and, during the calculations, on the phase-object images.

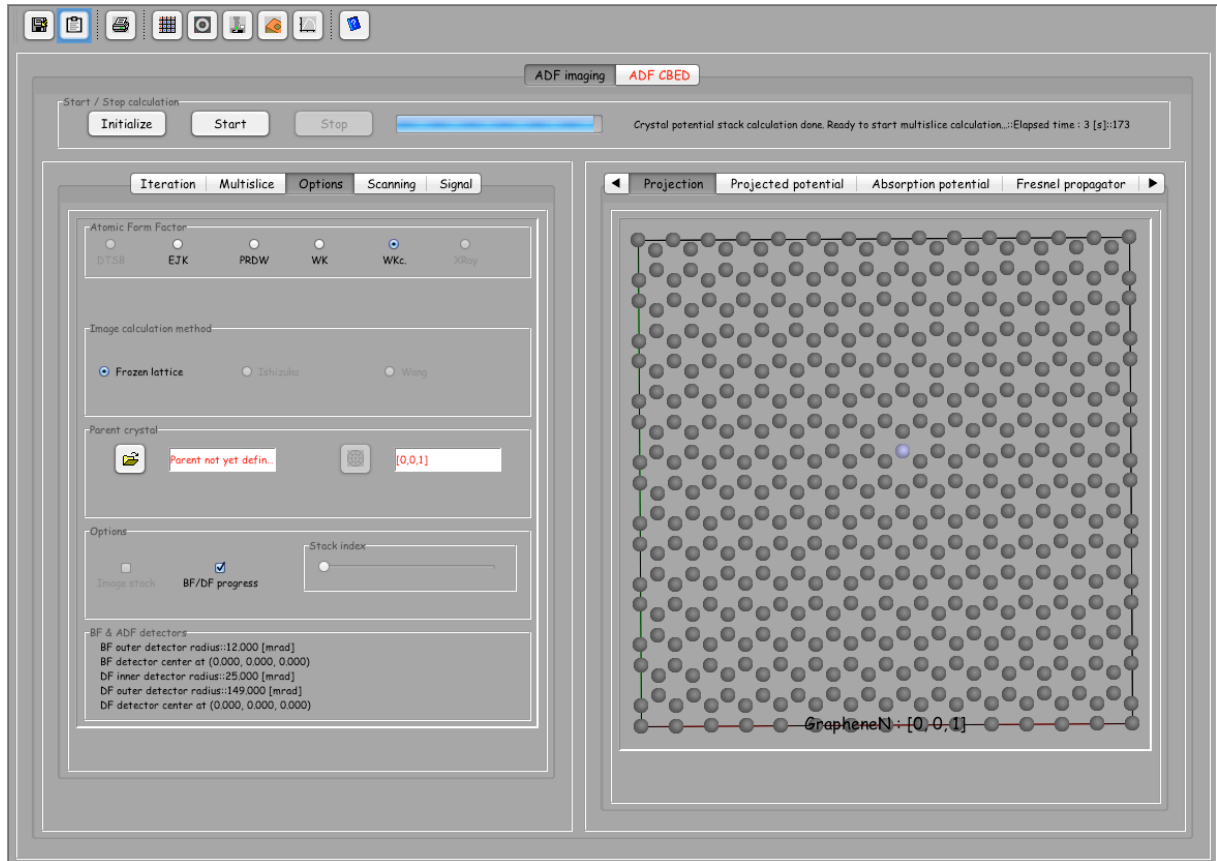


Figure 36: Model's slices tab.

4.6 Projected potential tab

The projected potential of the selected slice is displayed in this tab (Fig. 37).

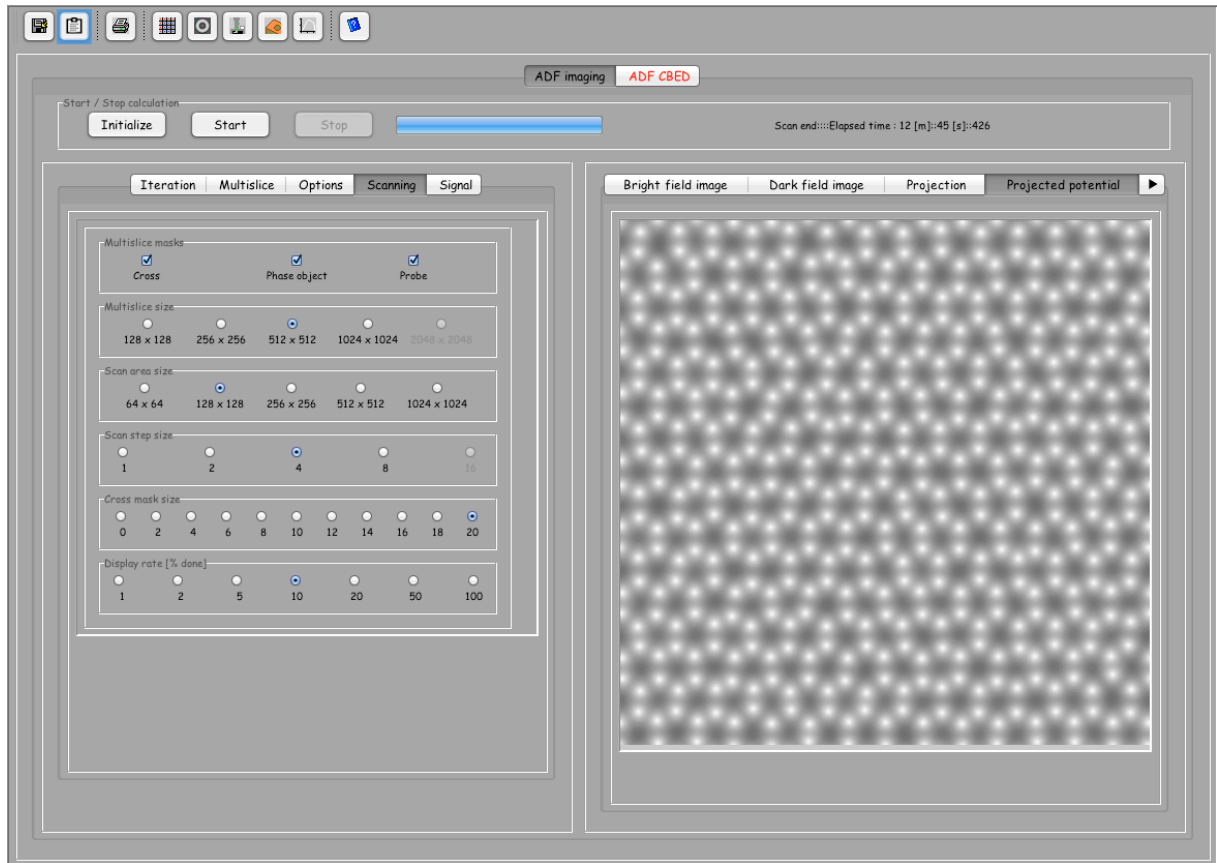


Figure 37: Projected potential tab.

4.7 Absorption potential tab

The absorption potential takes into account inelastic scattering events of plasmon or core origin (Fig. 38). It is best calculated using Weickenmeier-Kohl method (see 9.2). Absorption μ_{TDS} should not be included (though there are always some electrons scattered outside the detectors).

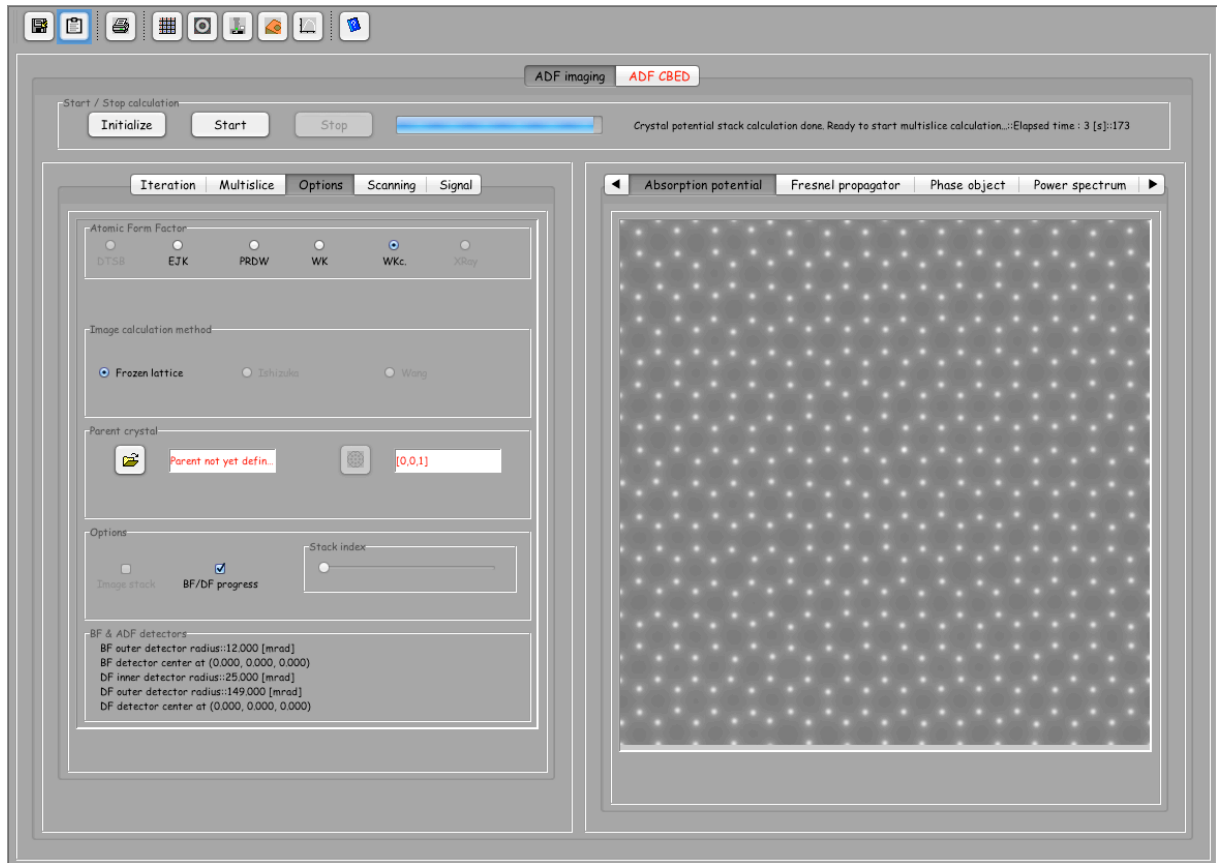


Figure 38: Absorption potential tab.

4.8 Fresnel propagator tab

This tab shows the Fourier transform of Fresnel propagator (Fig. 39) $FP(x, y; \Delta z)$ used by multislice method ($\overline{FP}(u, v; \Delta z)$). When the $O(\Delta z)$ approximation is selected, a multislice iteration cycle is performed as:

$$\Psi(x, y; z + \Delta z) = FP(x, y; \Delta z) \otimes (PO(x, y, \Delta z) \times \Psi(x, y; z))$$

When the $O(\Delta z^2)$ approximation is selected, a multislice iteration cycle is performed as:

$$\Psi(x, y; z + \Delta z) = FP(x, y; \frac{\Delta z}{2}) \otimes \left[PO(x, y, \Delta z) \times \left(FP(x, y; \frac{\Delta z}{2}) \otimes \Psi(x, y; z) \right) \right]$$

The convolution $FP \otimes$ is performed using a direct Fourier transform, a multiplication and an inverse Fourier transform. The $O(\Delta z^2)$ requires twice the number of Fourier transforms of the $O(\Delta z)$.

Note that a small crystal tilt can be introduced ($\approx 1 - 2$ degrees) can be introduced using the specimen dialogue (tilting the Ewald sphere).

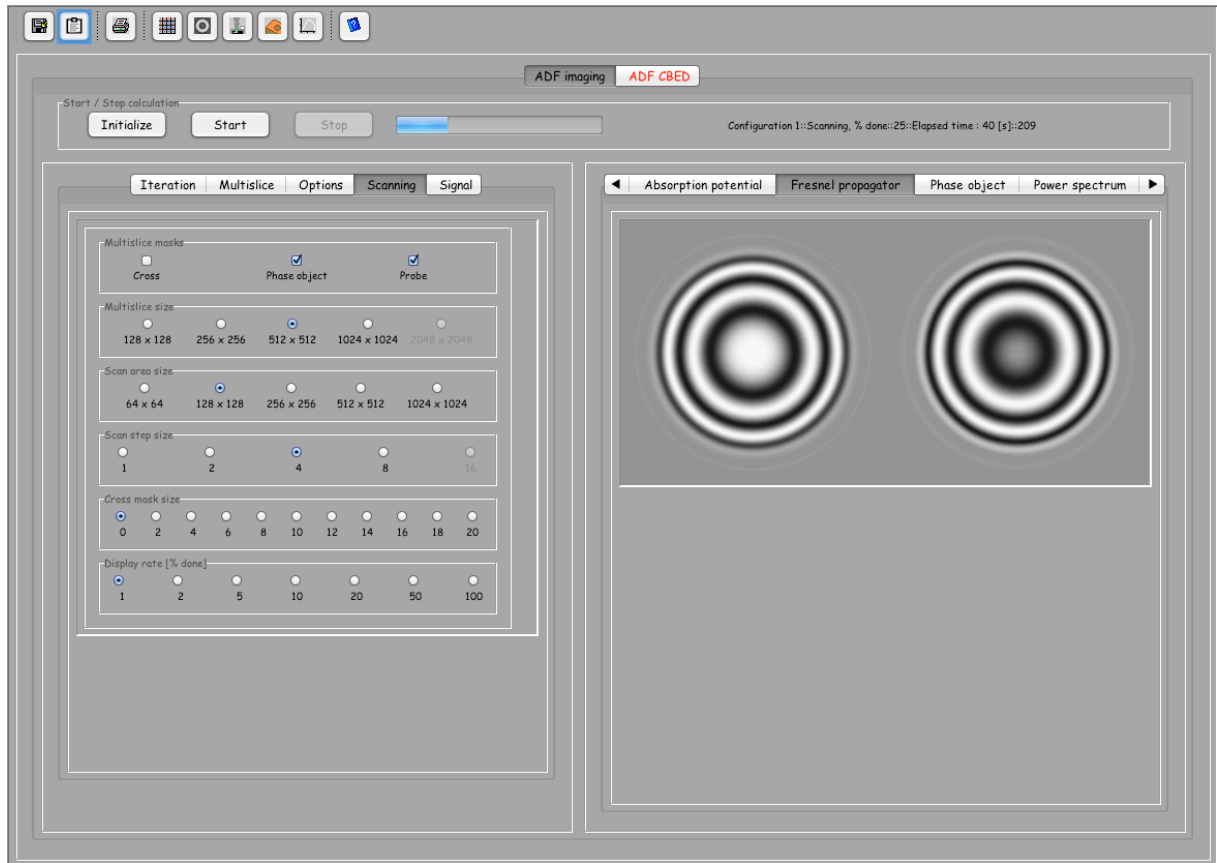


Figure 39: Fresnel propagator tab. The Fresnel propagator, $FP(x, y, \Delta z)$, is shown as $\overline{FP}(u, v; \Delta z)$.

4.9 Phase-object tab

The phase-object ($PO(x, y, \Delta z)$) is only displayed during the multislice iterations (real part on the left and imaginary part on the right, Fig. 40).

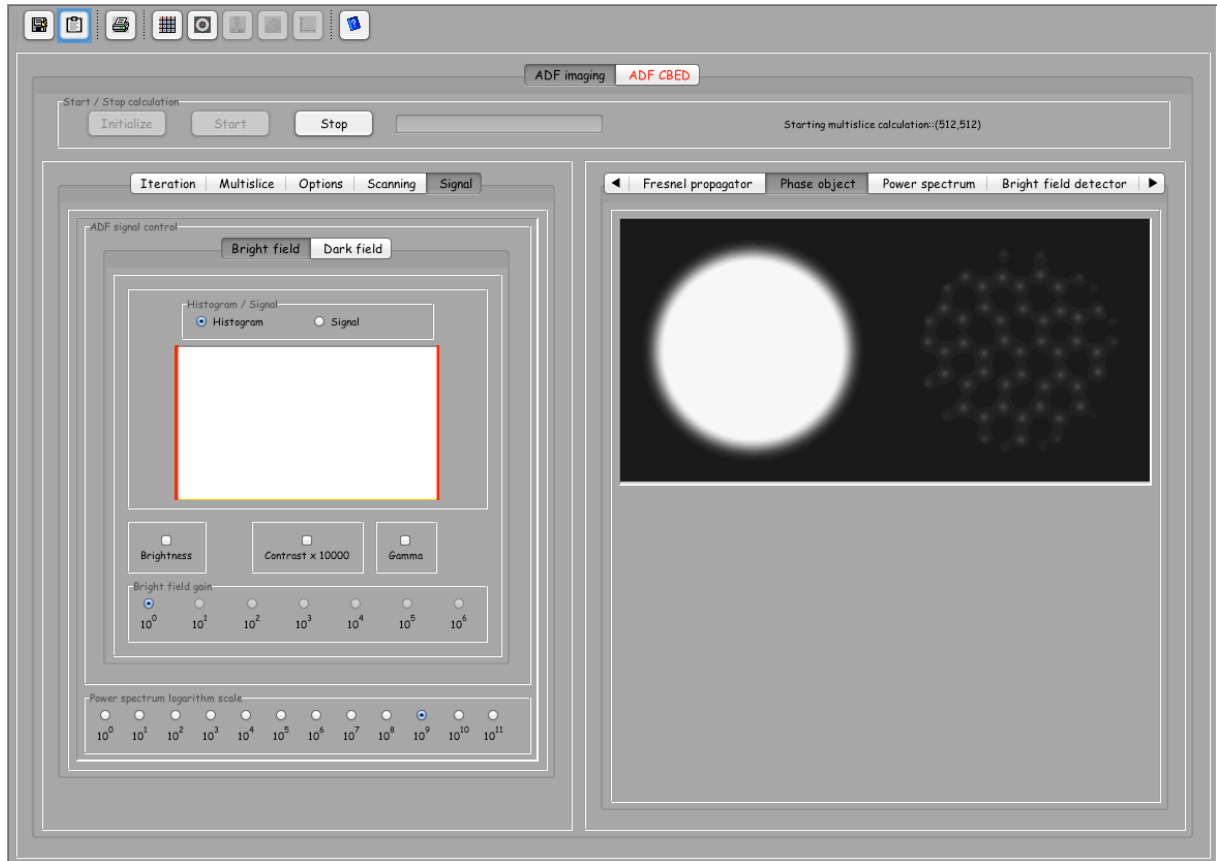


Figure 40: Phase-object tab. The phase-object, $PO(x, y, \Delta z)$ is shown here multiplied by a mask.

4.10 Power spectrum tab

The power spectrum ($PS(u, v)$) of the wave-function, $\Psi(x - x_o, y - y_o)$, at a given scan position (x_o, y_o) is shown in this tab (Fig. 41). The intensity can be premultiplied by a *Power spectrum logarithm scale* (see **Signal** tab).

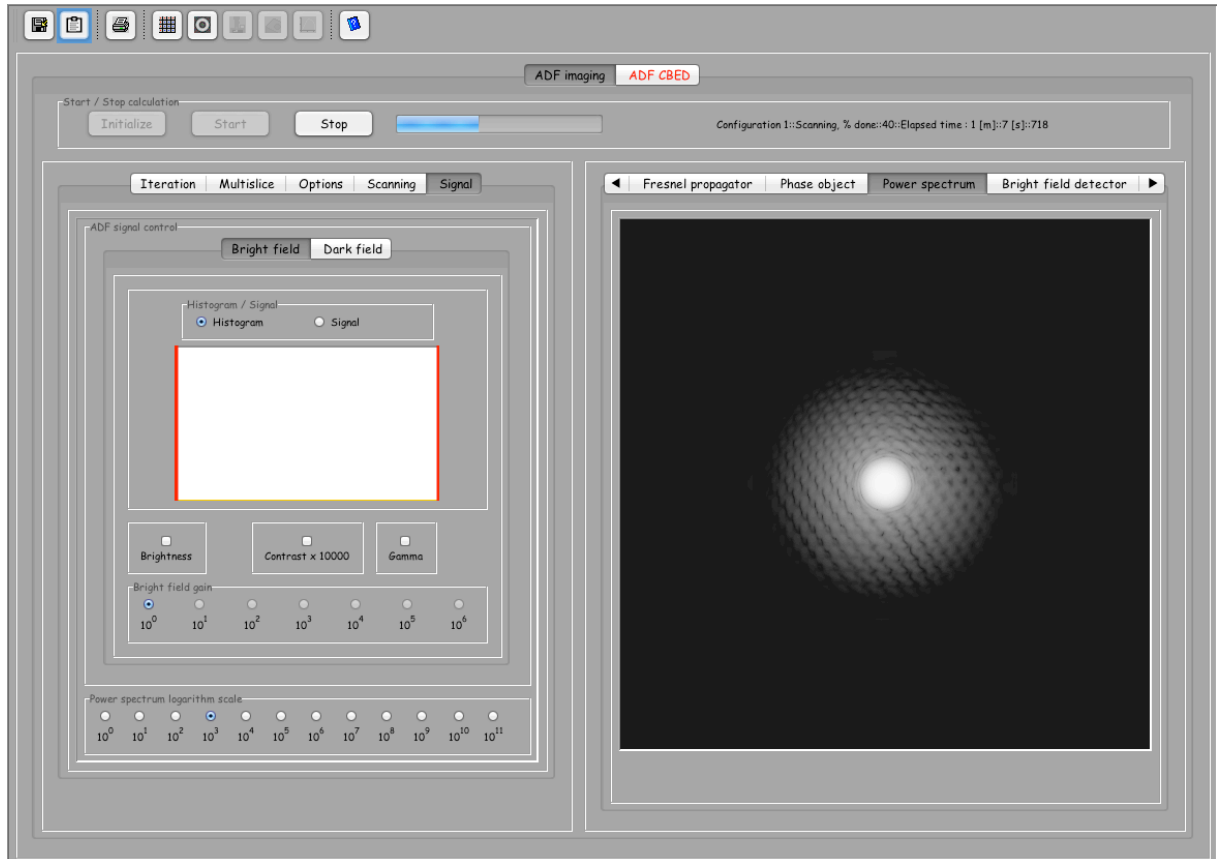


Figure 41: Power spectrum tab shows the logarithm of the whole power spectrum ($PS(u, v)$).

The logarithm of the whole power spectrum, $PS(u, v)$, can be premultiplied by a scaling factor in order to enhance the intensity of high spatial frequency reflections.

4.11 Bright-field detector tab

The signal collected by the **BF detector** is displayed in this tab (Fig 42).

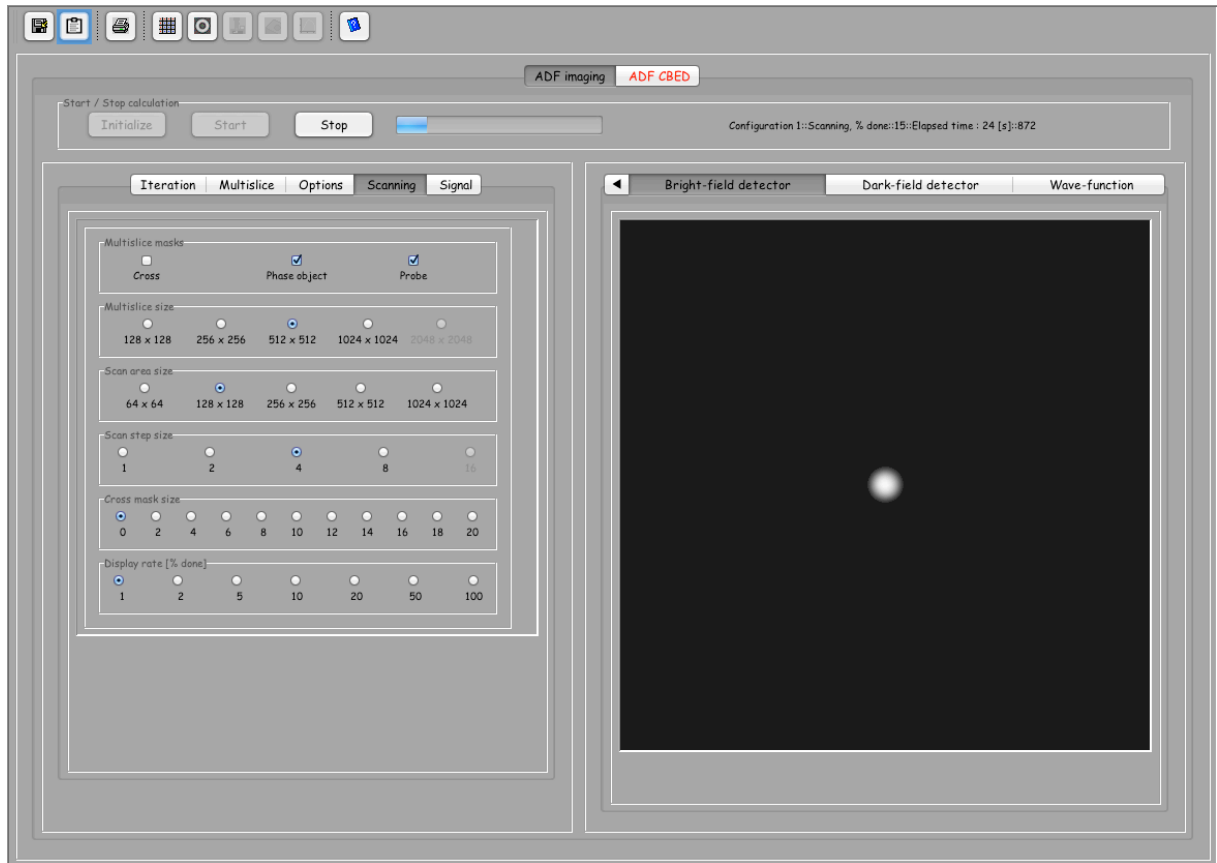


Figure 42: Bright-field detector tab. Portion of $PS(u, v)$ collected by the BF detector.

4.12 Dark-field detector tab

The signal collected by the **DF detector** is displayed in this tab as the logarithm of its intensity (Fig. 43). It can be premultiplied by a large factor in order to better display the inelastically scattering intensity.

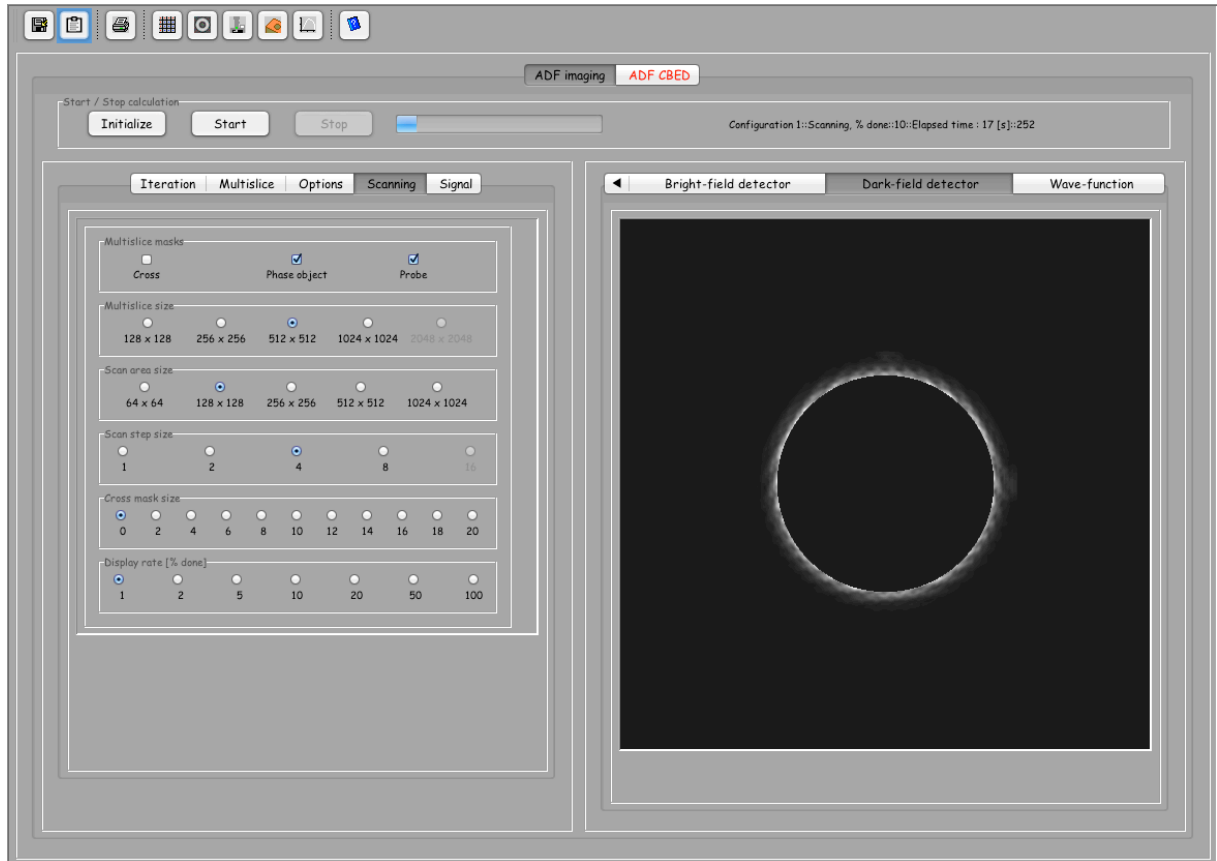


Figure 43: Dark-field detector tab. Portion of $PS(u, v)$ collected by the DF detector.

4.13 Sectors detector tab

The imaginary part wave-function, $\Psi(x, y)$, is shown in this tab (Fig. 44).

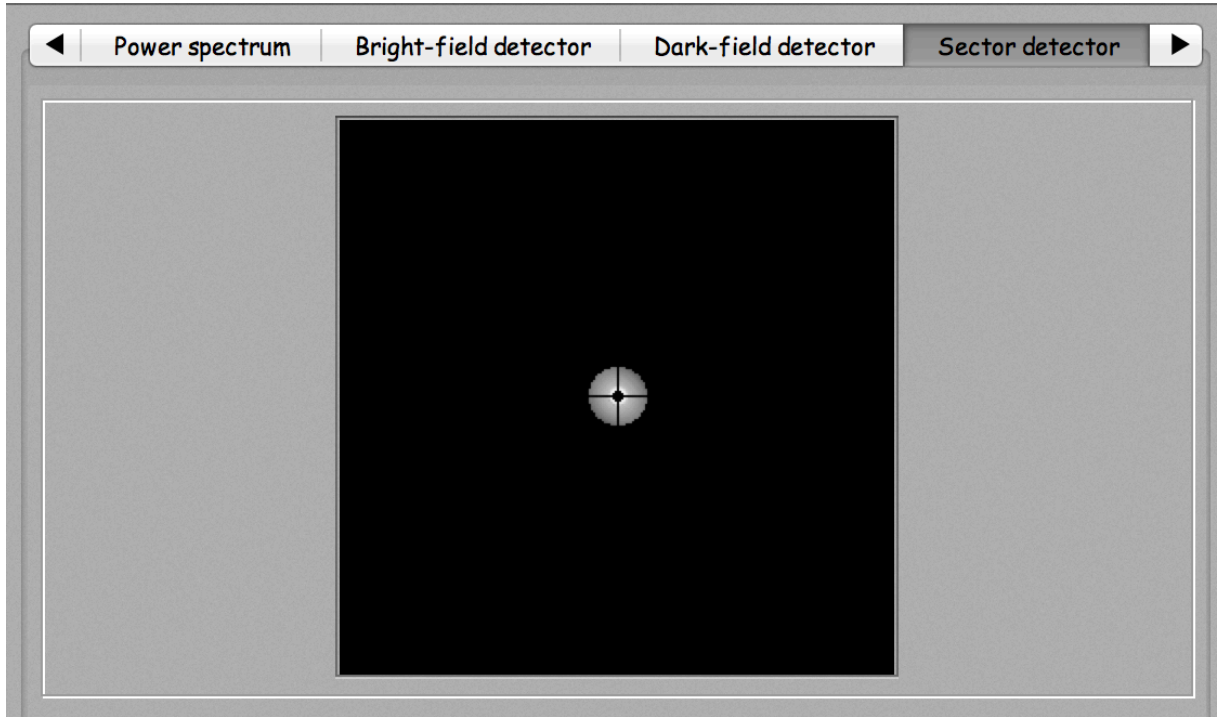


Figure 44: Sectors detectors tab. The sectors detector inner- and outer- radii are defined by the outer-radius of BF_1 and the inner-radius of ADf_1 . The inner-radius can be larger than the outer-radius of BF_1 and smaller than the inner-radius of ADf_1 .

4.14 Wave-function tab

The imaginary part wave-function, $\Psi(x, y)$, is shown in this tab (Fig. 45).

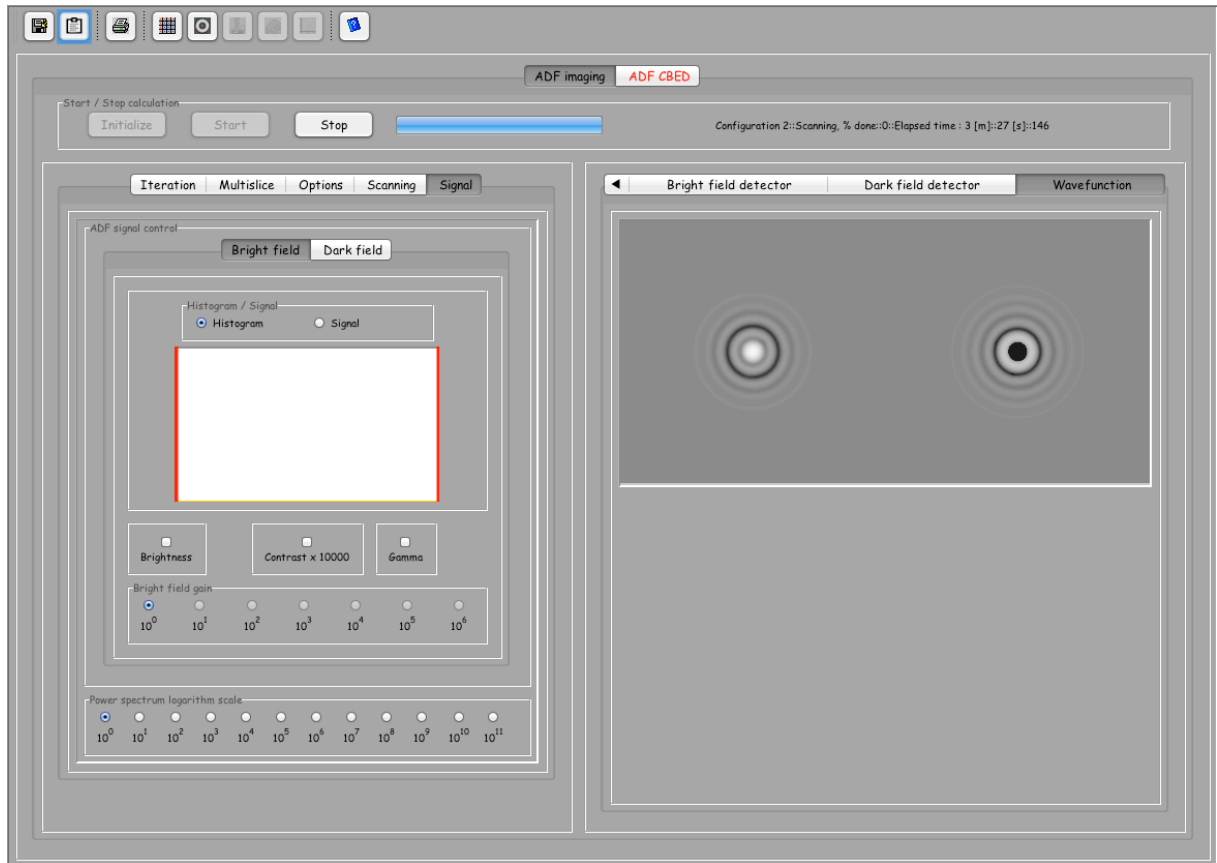


Figure 45: Wave-function tab. Imaginary part of $\Psi(x, y)$ at the bottom of the last slice of the model.

5 Probe imager dialogue

After complete initialisation, the **Start** button is enabled and the calculation can be started. The **Probe imager dialogue** will popup (Fig. 46). This dialogue allows to define the scan area position (when smaller than the phase-object size) and the probe shape. The probe shape depends on defocus, virtual objective aperture size (or convergence defined by C_2/C_3) and source size. Aberrations up to order 8 can be introduced (i.e. C78, A7 or W88). The aperture size can be displayed as $[nm^{-1}]$ or $[mrad]$ (see note 9.4).

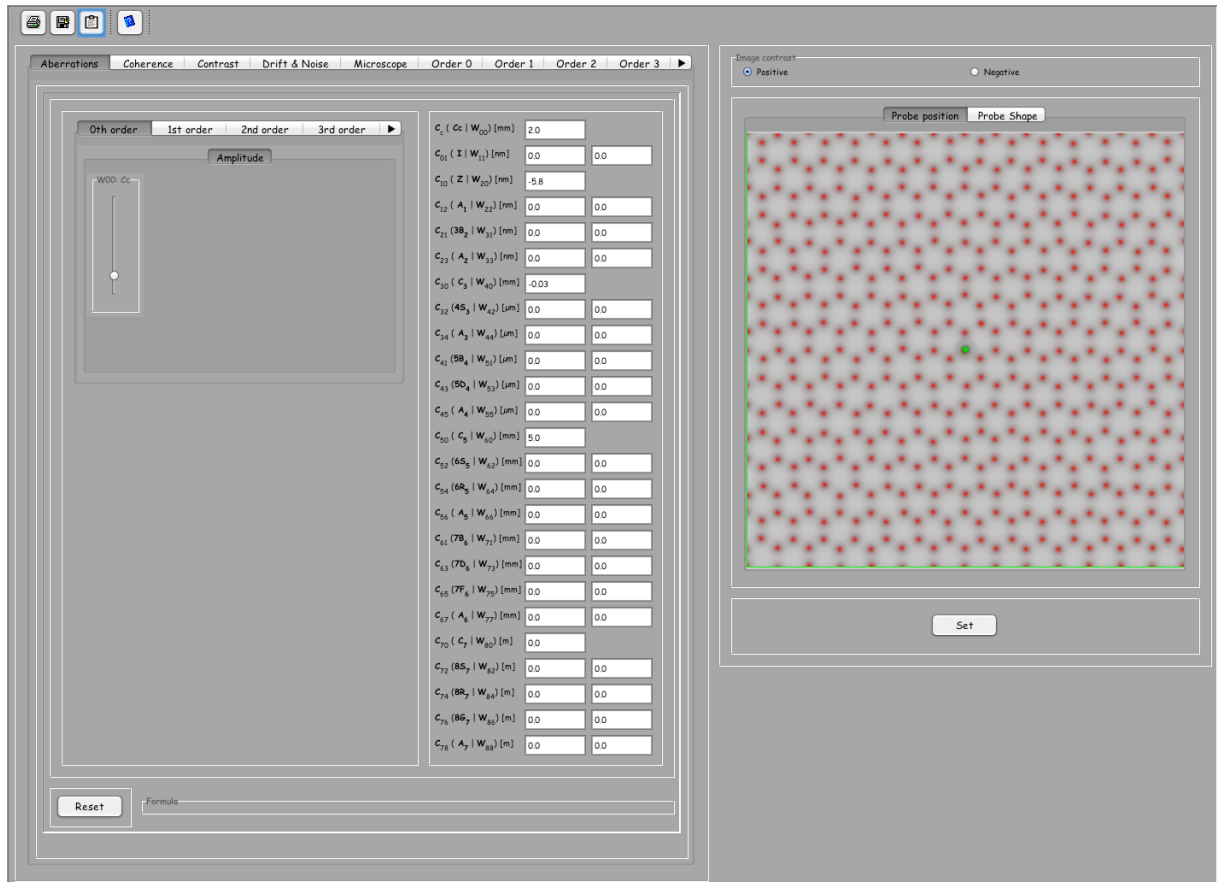


Figure 46: Probe imager dialogue. The scan area (square) and probe position are selected using the pointing device, i.e. usually mouse.

5.1 Scan area and probe position

The probe is shown at the centre of the scan area (Fig. 47). It is moved using the pointer or the mouse. The probe shape (Fig. 48 and 49) is adjusted using the controls of the probe imager dialogue left tab.

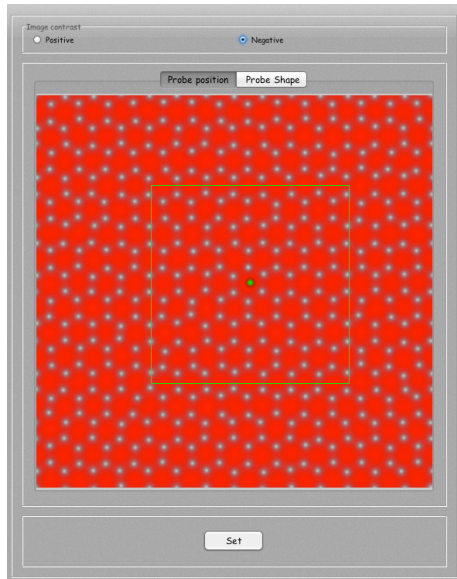


Figure 47: Scan area and probe position.

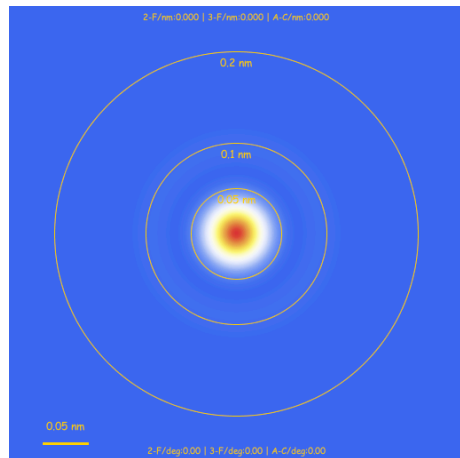


Figure 48: Probe shape with dimension circles.

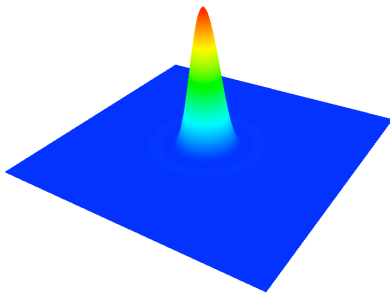


Figure 49: Probe shape 3-D.

The probe size is adjusted using the defocus, the **Aperture diam.** and the **Source size** controls. **Coherent** and **Envelope** illumination approximation can

be selected respectively. The aperture radius and source size controls are found in the **Microscope** tab (Fig. 50). Note that most of the sliders have a popup menu that allows to set its *Minimum*, *Maximum* or *Default* value. The popup menus of the **Aperture diam.** (and **Beam half conv.**) sliders allow to change the unit from [*mrad*] to [*nm⁻¹*] or from [*nm⁻¹*] to [*mrad*].



Figure 50: Adjusting the probe size.

6 Setting the bright-, dark-field and sectors detectors

Before selecting the bright-field and dark-field detectors size (equivalent to adjusting the diffraction camera length), it is suggested to define the "Single unit cell parent crystal", and the $[u,v,w]$ observation direction equivalent to the model $[0,0,1]$ observation direction. For graphene, the **graphite** unit cell and $[0,0,1]$ observation direction are selected (Fig. 51). The *Bright-field* controls adjust the camera length used to display the SAED pattern and the outer-radius of the BF detector (Fig. 52).

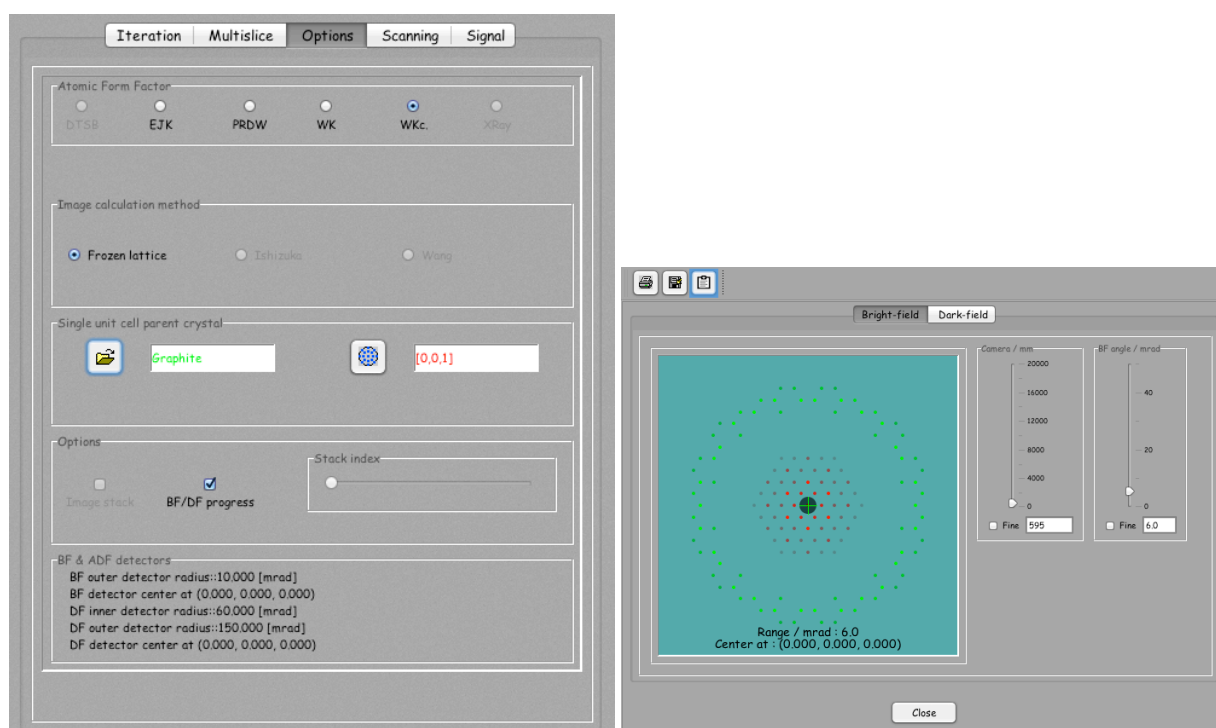


Figure 51: Parent crystal settings: graphite unit cell and $[0,0,1]$ observation direction. Figure 52: Detectors selector: bright-field detector tab allows to adjust the diffraction camera length and the bright-field detector angle ([mrad]).

The inner- and outer-radii of the dark-field detector are adjusted similarly using the **Dark-field** tab (Fig. 53). When the parent crystal is defined, the reflections of the first-order Laue zone are easily identified and a DF detector inner-radius

can be adjusted in order to avoid them ¹⁴ (Fig. 54). BF and DF sizes can be adjusted during the calculations.

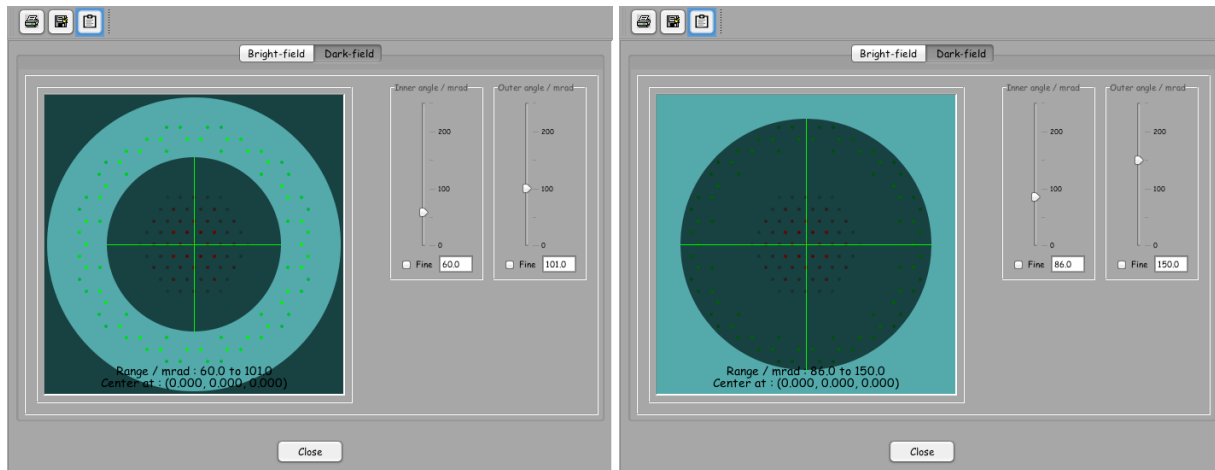


Figure 53: Dark-field detector selection using inner- and outer-radii ([mrad]).

Figure 54: Inner- and outer-radii of 86 and 150 ([mrad]) are necessary to avoid first-order Laue zone reflections.

¹⁴Note that a graphene sheet doesn't generate first order reflections.

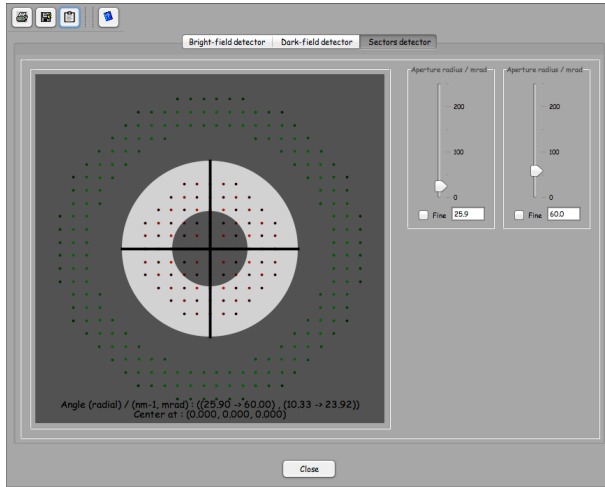


Figure 55: Sectors detector selection using inner- and outer-radii ([mrad]).

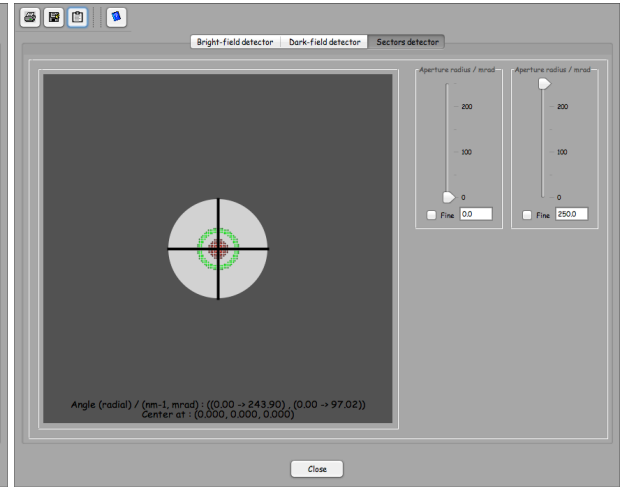


Figure 56: Sectors detector can be made very large by decreasing the BF detector outer-radius and increasing the DF detector inner-radius.

7 Doing a bright- or dark-field and sectors image calculation

In order to perform BF, DF and SE images calculations do the following:

1. Prepare the model and slice it into slices not thicker than ≈ 0.2 nm.
2. Start jems and load slice *somename_0000.txt*.
3. Start the ADF imager dialogue and load the series of slices from *somename_0001.txt*.
4. Set the ADF calculations parameters using the controls in tabs **Multislice** to **Signal**.
5. Push the **Initialize** button to initialise the phase-object, Fresnel propagator stacks.
6. Push the **Start** button when enabled. The **Stop** button aborts the calculation.

The detectors sizes (either in *mrad* or nm^{-1} units and their common center, shown as (hkl) indices of the ZOLZ, are displayed on the option tabs where BF_i are the bright-field detectors 1 to 4, ADF_i are the dark-field detectors 1 to 4 and SD the

sectors detector.

```
BF1 outer detector radius:: 25.0 [mrad] (9.97 [nm-1])
SD inner detector radius:: 25.9 [mrad] (10.33 [nm-1])
SD outer detector radius:: 60.0 [mrad] (23.92 [nm-1])
ADF1 inner detector radius:: 60.0 [mrad] (23.92 [nm-1])
ADF1 outer detector radius:: 117.4 [mrad] (46.78 [nm-1])
BFi (2 <=i<= 4) = BF1 + (i - 1) 5.0 [mrad]
ADFi (2 <=i<= 4) = ADF1 + (i - 1) 10.0 [mrad]
BF/ADF/SD detectors center::(0.000, 0.000, 0.000)
```

You might have to introduce the **Cross** mask in order to cancel weak multislice artefacts (see note 9.5). Assuming an isotropic radial distribution of intensity on the **Dark field** detector, the intensity collected by this detector is reduced by a factor that is display in the console together with the area of the BF and DF detectors (as a fraction of the power spectrum area).

Without the **Cross** mask:

```
BF detector area [a.u.] = 0.0036172867
DF detector area [a.u.] = 0.06423378
```

Without a **Cross** mask of 23 pixels width that cancels most of the multislice artefacts:

```
BF detector area [a.u.] = 0.0036172867
DF detector area [a.u.] = 0.06423378
DF detector + cross wire area [a.u.] = 0.056114197
```

8 Example: GaAs [110]

Figures 57 and 58 show the stack of slices and the 3-D model for calculating BF and DF images (GaAs [110]). The GaAs model is prepared using **Make orthogonal (Crystal)**. The GaAs [110] unit cell is then duplicated using **To triclinic** (menu **Miscellany**) and finally sliced in 4 slices of ≈ 0.2 nm thick slices using **To slices** (menu **Miscellany**).

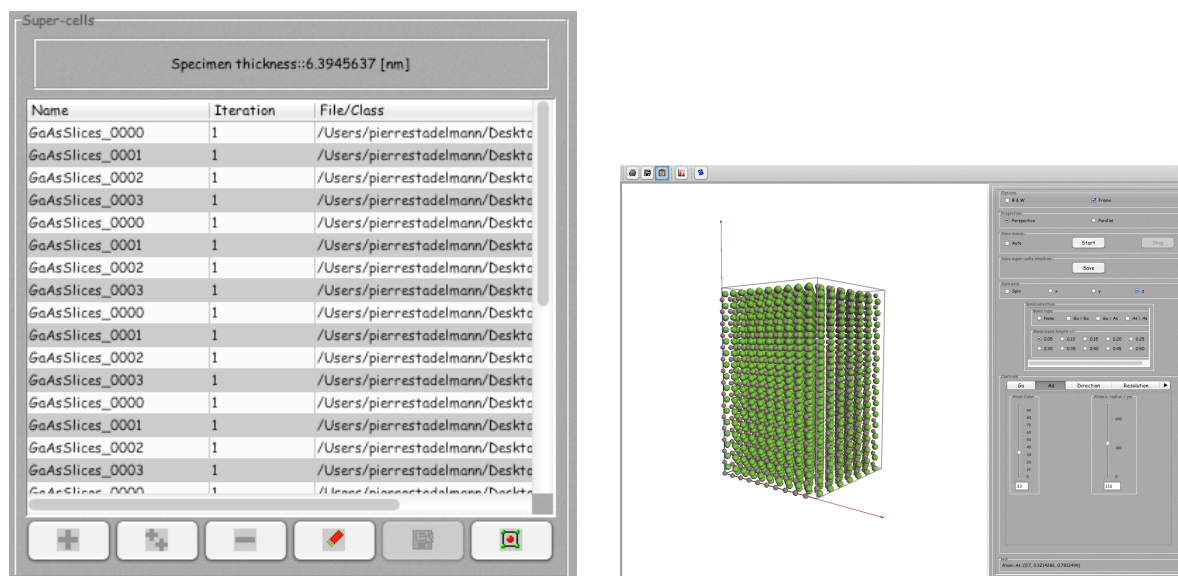


Figure 57: GaAs [110] stack of slices (8×4 slices). Total model thickness is $8 \times 0.79 = 6.3$ nm.

Figs. 59 and 60 show BF and DF images stacks. Fig. 64 shows a profile plot across the Ga and As atoms position. Only 2 atomic configurations have been used for this 512×512 multislice calculation, scan size of 64×64 , 32 slices (calculation time is ≈ 1 hour, Intel i7, iMac).

BF and DF images using a 256×256 calculation, performed in ≈ 10 minutes, are shown in Figs. 62 and 63. It is advised to start with calculations of small sizes and to increase their size when absolutely needed (i.e. for quantitative purposes).

Doing 512×512 simulations takes much more computer time (several hours or days). The next figures show some dark-field images of GaAs [110] and different dark-fielded detector sizes. It should be noted that the detector outer-radius must not be larger than $2/3$ of the maximum spatial frequency imposed by the anti-aliasing that depends on the multislice calculation size. Also since the ADF images is

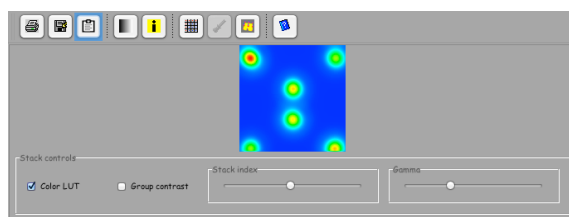
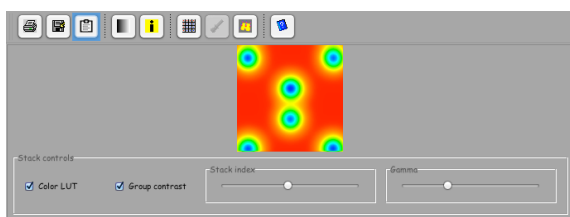


Figure 59: GaAs [110], BF image stack (512 × 512 multislice calculation), BF detector radius 10 mrad. Figure 60: GaAs [110], DF image stack (512 × 512 multislice calculation), DF detector inner- and outer-radius 60 - 185 mrad.

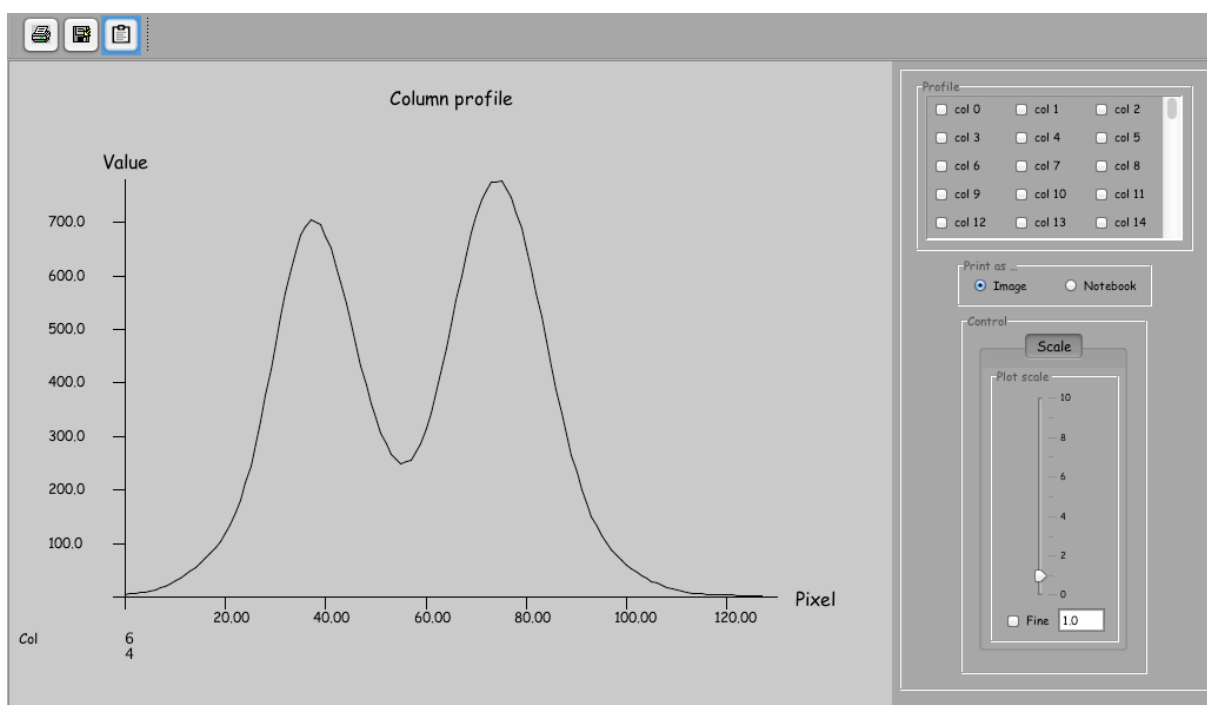


Figure 61: Intensity profile across Ga and As atoms (512 × 512 multislice calculation).

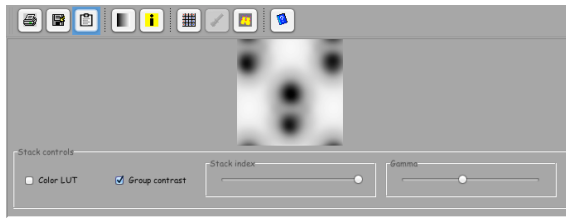


Figure 62: GaAs BF (256×256 multislice calculation). Note that scan area is not identical to previous BF image (Fig. 59).

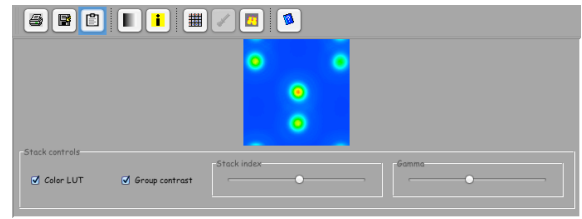


Figure 63: GaAs BF (256×256 multislice calculation). Note that scan area is not identical to previous DF image (Fig. 60).

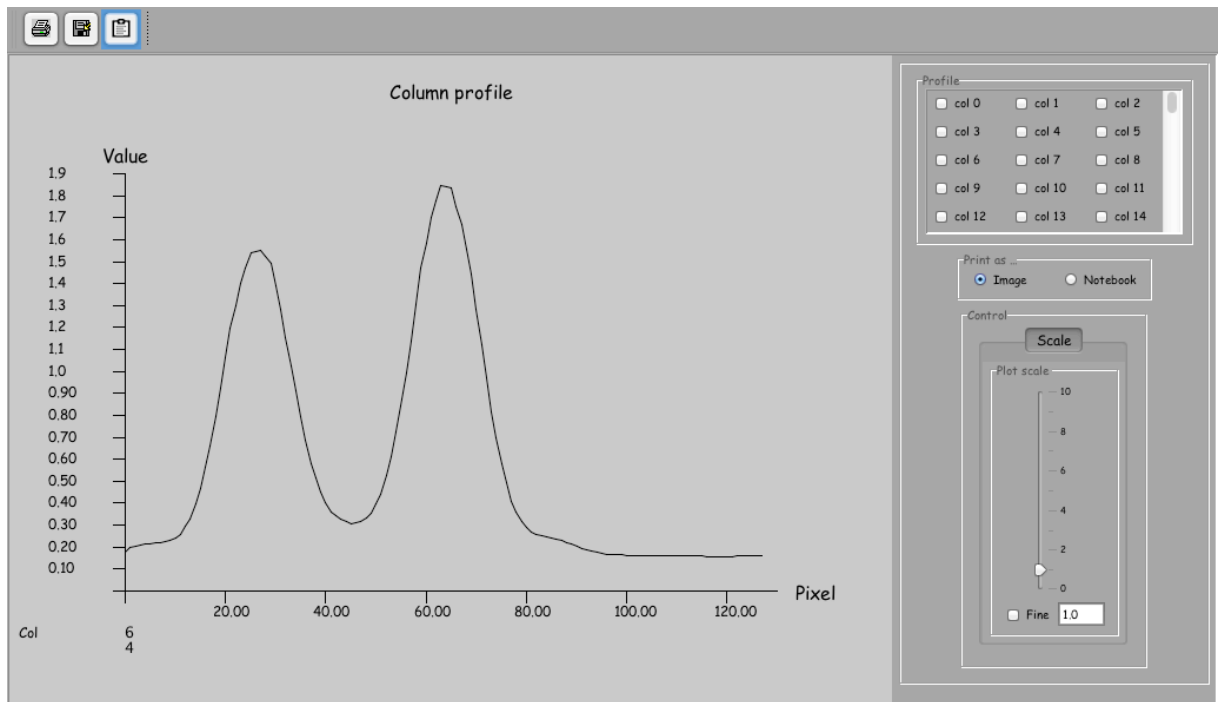
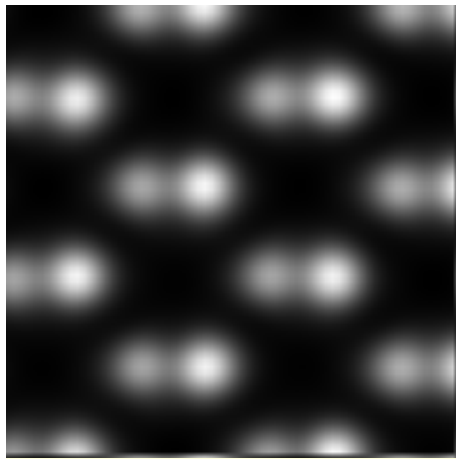
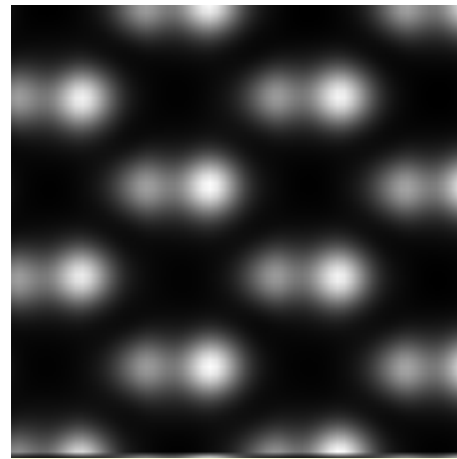


Figure 64: Intensity profile across Ga and As atoms (256×256 multislice calculation). Note that the qualitative agreement is fair for $6 \times$ shorter calculation time.

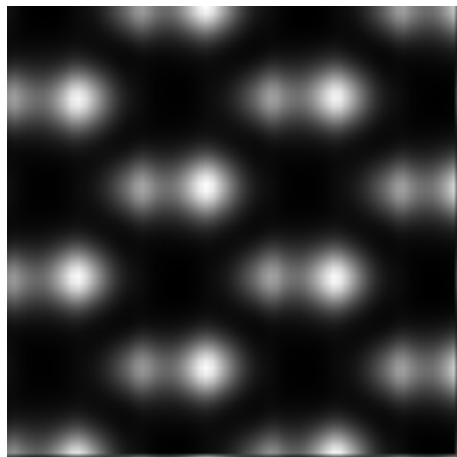
using single precision floating point numbers the accumulation of rounding errors finally makes the errors of large image spatial frequencies as large as the TDS signal. This effect can be observed on the images Fig. ??fig:ADFDetector1 to ??fig:ADFDetector4 where the GaAs crystal thickness is 51 nm (256 slices of 0.2 nm). Possible solutions would be to do 1024x1024 multislice calculation or to perform simulation using double precision floating point numbers. Note also that Kikuchi lines are visible on the power spectrum image that is only calculated with a single atomic configuration (Fig.66(a)).



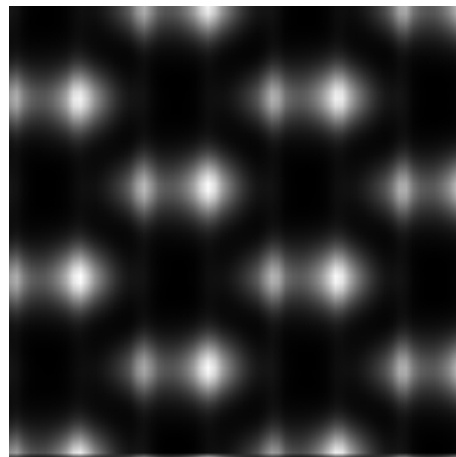
(a) ADF detector inner- and outer radius: 60, 150 mrad.



(b) ADF detector inner- and outer radius: 75, 165 mrad

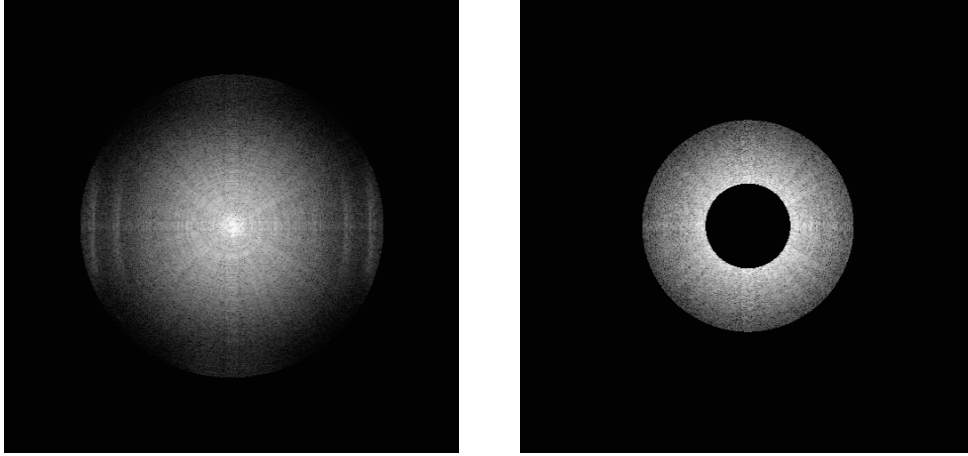


(c) ADF detector inner- and outer radius: 90, 180 mrad (too large for thicknesses larger than 35 nm)



(d) ADF detector inner- and outer radius: 105, 195 mrad (too large for thicknesses larger than 25 nm)

Figure 65: Image artefacts introduced by large outer-radius ADF detector (150 to 195).



(a) Power spectrum (1 atomic configuration) 55 nm thick GaAs.

(b) ADF detector inner- and outer-radius: 60, 150 mrad

Figure 66: Rounding or aliasing errors are accumulating perpendicularly to the GaAs dumbbells (GaAs [110]).

9 Notes

9.1 Note 1: Debye-Waller temperature factor

The Debye-Waller temperature factor M_k is given by $M_k = 8\pi^2 \langle u^2 \rangle_k$, where $\langle u^2 \rangle_k$ is the mean-square vibrational amplitude of atom k in the unit cell. In the Debye model for lattice vibrations, a linear dispersion relationship is assumed and the excitation spectrum is parameterized using the Debye-temperature θ_D :

$$\langle u^2 \rangle = \frac{3h^2}{4\pi^2 m_k \theta_D} \left(\frac{1}{4} + \frac{T^2}{\theta_D^2} \int_0^{T/\theta_D} \frac{x}{e^x - 1} dx \right)$$

where m_k is the mass of atom k .

Using the harmonic approximation for the vibration of the atoms, the temperature dependence of $\langle u^2 \rangle$ is given by:

$$\langle u^2 \rangle = \frac{\hbar}{2m} \int_0^{\omega_m} \coth \left(\frac{\hbar\omega}{2k_B T} \right) \frac{g(\omega)}{\omega} d\omega$$

where $g(\omega)$ is the normalized phonon density of states and ω_m the maximum phonon frequency. Using either the Debye- or the Einstein model for lattice vibration, it is found that for high temperatures $\langle u^2 \rangle$ is a linear function of temperature.

9.2 Note 2: calculation of the atomic scattering amplitude

The atomic scattering amplitude for electrons $f^B(g)$ has been given in analytical form by Weickenmeier and Kohl¹⁵:

$$f^B(s) = \frac{1}{s^2} \sum_{i=1}^6 A_i \left[1 - e^{-B_i s^2} \right] \quad s = g/4\pi$$

where the A_i and B_i are tabulated for atomic number 1 to 92. Options WK_c also includes core absorption.

The projected potential is computed in 3 possible ways:

1. *Analytic* The projected potential of an atom is described by an analytic function of its (x, y) position.
2. *Direct* The atom potential is calculated, integrated over z and patched at its (x, y) position.
3. *Fourier* The Fourier transform of the projected potential is computed and then inverse Fourier transform. It is the most accurate method, but also the slowest.

9.3 Note 3: absorption coefficient μ_{TDS}

$$\mu_{TDS} = \frac{1}{k_0^2 \Omega_0} \sum_a \int d\sigma(\tau) |f_a^B(\tau)|^2 (1 - e^{-2W_a(\tau)})$$

where k_0 is the incident wave vector. Ω_0 the volume of an atom and $e^{-W_a(\tau)}$ the Debye-Waller factor of atom a. The surface integral is taken from the inner edge of the dark-field detector to infinity. This formulation allows to calculate the TDS intensity falling on the dark-field detector within K. Ishizuka approximation.

9.4 Note 4: popup menu attached to slider controls

A popup menu is attached to most sliders. It is displayed as all popup menus are, i.e. with a right button click or a double click when the mouse or pointer is placed

¹⁵A. Weickenmeier and H. Kohl. Computation of Absorptive Form Factors for High-Energy Electron Diffraction. Acta Cryst. A47:590-597, 1991.

on the slider handle (Figs. 67 and 68). Slider of Fig. 68 allows to switch between $[mrad]$ and $[nm^{-1}]$ units.

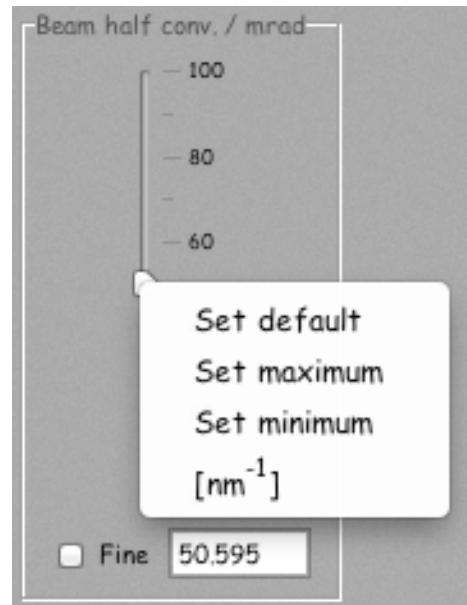
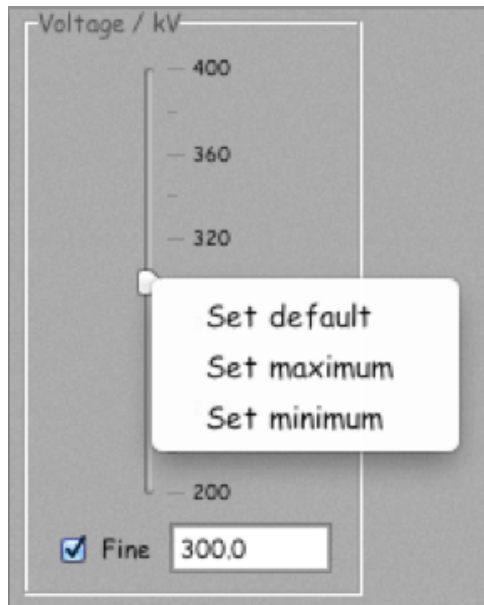


Figure 67: Standard slider popup menu.

Figure 68: Popup menu allowing to switch from $[mrad]$ to $[nm^{-1}]$ unit (here $[mrad]$ are selected).

9.5 Note 5: sampling artefacts

Though all the calculations are performed in double precision, due to the discrete nature of the multislice method, calculation artefacts could appear centred as weak intensity bands centred at spatial frequency $(0, 0)$ and distributed in the O_u (horizontal) or O_v (vertical) directions. These artefacts are visible when a high DF signal gain is set.

The intensity falling on the DF detector is show in Fig. 69. The df_{signal} gain (df_{gain}), defined in the **Signal** tab, is 10^9 and a logarithm scale is used to display the intensity:

$$\log [1 + df_{gain} \times df_{signal}]$$

In Fig. 70 the intensity is shown as:

$$\log [1 + 10^6 \times df_{gain} \times df_{signal}]$$

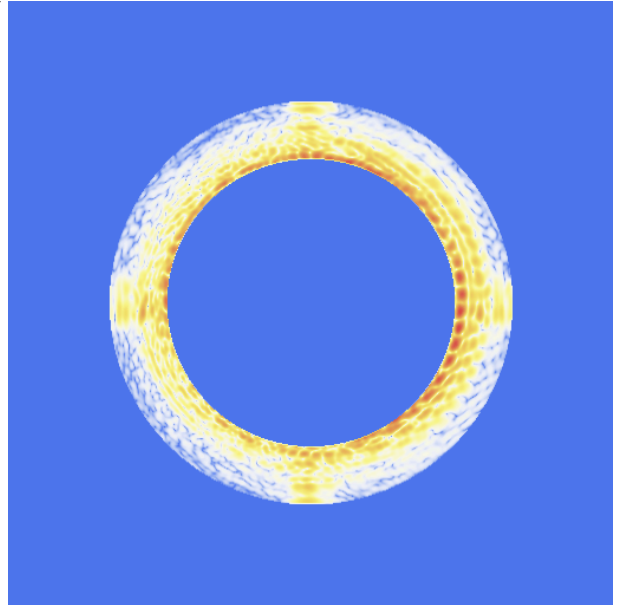


Figure 69: DF detector, dark-field signal gain is 10^9 , logarithm scale = 1.

Figure 70: DF detector, dark-field signal gain is 10^9 , logarithm scale = 10^9 . The combined df signal gain is 10^{15} , i.e. matching the double precision error ($2^{-53} = 1.11 \times 10^{-16}$).

i.e. a 10^{15} df_{gain} makes the sampling artefacts visible. The 10^6 factor is selected at the bottom of the **Signal** tab.

The calculation artefacts can be eliminated (and quantified) by placing a cross mask in front of the DF-detector (Fig. 71 and 72). The width of the cross bars is adjusted by using a set of radio buttons.

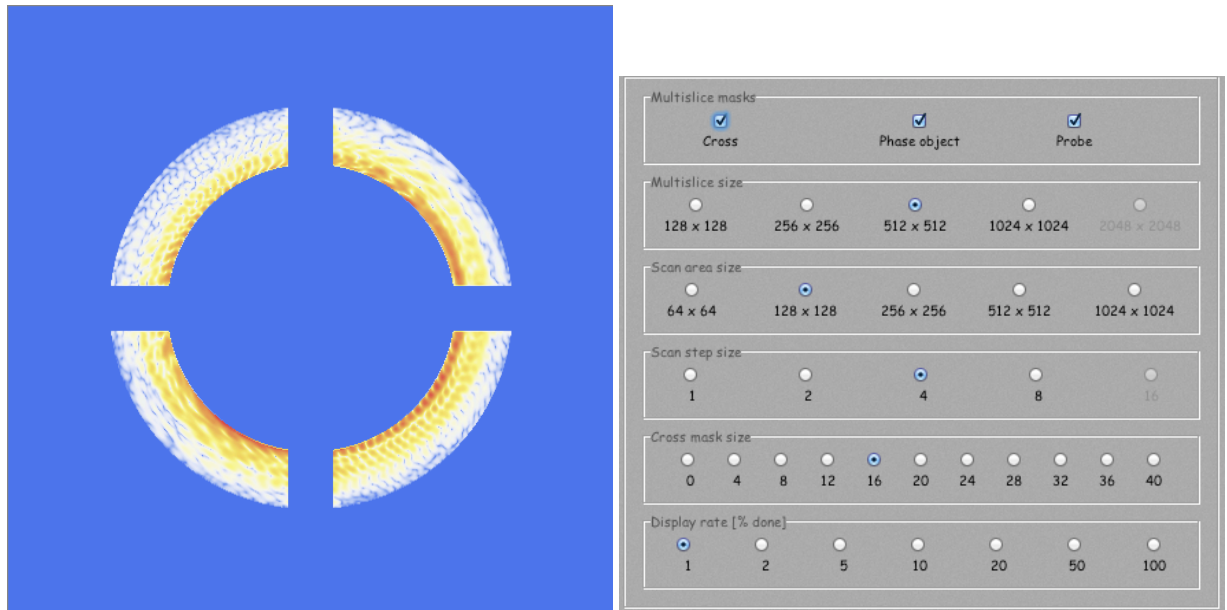


Figure 71: A cross placed in front of the DF detector masks the artefacts.

Figure 72: The width of the cross bars selection. The minimum width is 3 pixels.